Analyst

ROYAL SOCIETY OF CHEMISTRY

CRITICAL REVIEW

View Article Online
View Journal | View Issue

Cite this: *Analyst*, 2024, **149**, 1680

Separation and purification of fluorescent carbon dots – an unmet challenge

Namratha Ullal, Riya Mehta and Dhanya Sunil *

Literature reports demonstrate versatile optical applications of fluorescent carbon dots (CDs) in biological imaging, full-color solid-state lighting, optoelectronics, sensing, anticounterfeiting and so on. The fluorescence associated with CDs may originate significantly from byproducts generated during their synthesis, which need to be eliminated to achieve error-free results. The significance of purification, specifically for luminescence-based characterizations, is highly critical and imperative. Thus, there is a pressing demand to implement consistent and adequate purification strategies to reduce sample complexity and thereby realize reliable results that can provide a tactical steppingstone towards the advancement of CDs as next-generation optical materials. The article focuses on the mechanism of origin of fluorescence from CDs and further demonstrates the different purification approaches including dialysis, centrifugation, filtration, solvent extraction, chromatography, and electrophoresis that have been adopted by various researchers. Furthermore, the fundamental separation mechanism, as well as the advantages and limitations of each of these purification techniques are discussed. The article finally provides the critical challenges of these purification techniques that need to be overcome to obtain homogeneous CD fractions that demonstrate coherent and reliable optical features for suitable applications.

Received 10th December 2023,
Accepted 4th February 2024

DOI: 10.1039/d3an02134c

rsc.li/analyst

Introduction

Carbon dots (CDs) are zero-dimension quasi-spherical allotropes of carbon having a size below 10 nm that generally exhibit tunable photoluminescence characteristics. After their discovery as a byproduct during the synthesis of carbon nanotubes,[1] CDs are extensively studied for diverse applications including biosensing,[2–4] bioimaging,[5,6] optoelectronic devices,[7,8] solar cells[9,10] *etc*. The term CD is broad and is classified into different types, carbon quantum dots (CQDs),[11] graphene quantum dots (GQDs),[12] carbon nanodots (CNDs),[13] and carbonized polymer dots (CPDs),[14] based on their unique carbon core structure, surface functionalities, chemical, physical, and photophysical properties (Fig. 1).[15] CQDs are crystalline carbon nanoparticles with a core comprising a combination of sp^2 and sp^3 carbons, whereas GQDs are single- or multi-layered graphene particles with <10 nm size having chemical groups and graphene lattices at their edges. GQDs are composed dominantly of sp^2 carbon formed from π-conjugated graphene sheets, and display quantum confinement when these conjugated domains are separated by defects at the level of the graphene sheet. The edge effect is caused because of several chemical functional moieties present within the edge or interlayer defect.[16] Furthermore, graphene-like 2D graphitic carbon nitride quantum dots (g-CNQDs) are frequently referred to as equivalents of GQDs. The quasi-spherical CNDs are mostly made up of an amorphous structural core, devoid of a crystal lattice, whereas CPDs are carbonaceous nanoparticles with a central carbonized core surrounded by polymer chains or functional groups produced by the aggregation or crosslinking of linear monomers or polymers.[17]

Although there are dedicated and systematic reviews that focus on the synthesis methods, properties, and applications of CDs,[18–23] a distinct compilation of separation and purification techniques for CDs that influence their optical features is not available. Through this article, we aim to spotlight the mechanism of fluorescence origin in CDs, which is of prime importance as the optical properties are vital for their biological and optoelectronic applications. Furthermore, a sincere attempt has been made to specifically present the need for the purification of CDs and the various techniques adopted by several research groups for the separation of the as-synthesized carbonaceous nanoparticles. Besides, the article focuses not only on the fundamental separation mechanism, but also the advantages and drawbacks of each of the implemented purification strategies. Finally, the review extends to provide critical insights into the influence of purification techniques on the fluorescence of CDs and proposes future research that could be undertaken towards this direction.

Department of Chemistry, Manipal Institute of Technology, Manipal Academy of Higher Education, Manipal-576104, Karnataka, India.
E-mail: dhanyadss3@gmail.com

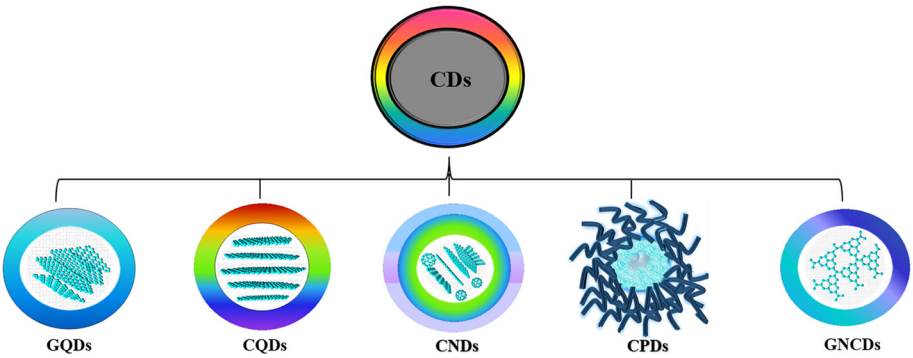

Fig. 1 Classification of CDs.[16]

Synthesis routes and fluorescence properties of CDs

The use of less expensive precursors and facile synthesis to realize CDs with different functionalization possibilities has garnered immense research attention.[22–26] The synthesis techniques adopted for CDs are broadly divided into 'top-down' and 'bottom-up' depending on the carbon source and the method adopted. The fluorescence emission of the CD sample generated is one of the most fascinating features, and has been exploited in versatile applications. The surface functional groups of the CDs could be changed by utilizing different synthesis routes to achieve tunable photoluminescence (PL).

The top-down method depends on cutting, stripping off or exfoliating bulk carbon into luminous nanoscale carbon materials of <10 nm size with high crystallinity, which can be further modified post-preparation. Top-down techniques include chemical oxidation, laser ablation, arc discharge, electrochemical approaches, and ultrasonic passivation. The chemical exfoliation process makes use of a variety of bulk carbon precursors, such as carbon fibers, graphene oxide, and graphite or multi-walled carbon nanotubes cleaved by oxidizing agents or strong acids. Making luminous CDs with different fluorescence emission and excitation-wavelength-dependent emission using this method is simple, rapid, and inexpensive because it does not require sophisticated equipment.[27–29] Laser ablation is practical and simple in using an intense laser pulse, which causes carbon vapors to crystallize into a range of nanostructures. Laser passivation has a significant influence on the PL performance and generates CDs with stable/visible/dual/tunable emission.[30] In arc-discharge methods the decomposition of the carbon precursor to form carbon vapors that assemble to fluorescent nanostructures occurs at high temperatures (>4000 K) when an electrical arc-discharge is formed between two metallic electrodes. Though CDs with high quality are obtained in this method, their yield is less. Electrochemical deposition occurs at the interface of an electrolyte solution containing the metal to be deposited and an electrically conductive metal substrate. In this case, strong emission arises from the quantum-sized graphite structure, and small, medium, and large CDs emit in the ultraviolet (UV), visible region, and near-infrared (NIR) regions.[11] In the low-cost and simple ultrasonic-assisted process, strong hydrodynamic shear forces generated from the cavitation of small bubbles cut macroscopic carbon materials into nanoscale pieces. The as-prepared CDs generally display good PL features with superior photostability.[31]

In the "bottom-up" approach, single atoms and molecules assemble into larger nanostructures of the required size with distinct optical characteristics and high quantum yield (QY). The bottom-up approaches including hydrothermal, microwave, plasma, pyrolysis/carbonisation *etc.* are more economical, have adjustable reaction conditions and are less harmful to the environment. Hydrothermal/solvothermal is one of the extensively used approaches, wherein the reactants in water/solvent are subjected to a high temperature and pressure to obtain CDs of a homogeneous size distribution. Natural and biowaste materials are used as precursors to obtain CDs with multifunctional PL properties, good QY, low toxicity and high photostability.[32] Microwave-assisted synthesis involves the use of intense energy to heat carbon precursors in a single step, to produce luminous CDs having good biocompatibility as well as high QY and photostability with excellent yield, but with poor regulation of the nanoparticle size.[33,34] Molecular precursors such as carbohydrates can be burned or heated at high temperature in the pyrolysis process to produce CDs. This process is advantageous in terms of easy operation, shorter reaction time, use of solvent-free methods, scalable production, and low cost. However, the resulting CDs have a wide size range and produce excitation-wavelength-dependent fluorescence emission, down- and up-conversion fluorescence, good PL stability and high solubility.[35–38]

Origin of fluorescence emission from CDs

Literature evidence provides exhaustive studies exploiting the fascinating PL behavior of CDs including excellent photostability, fluorescence in the visible or NIR region, tunable fluo-

rescence, excitation wavelength emission, efficient up-converted PL, and photoinduced electron transfer ability.[39] The facile synthesis of CDs as described in the previous section enables researchers to use different precursors such as synthetic molecules, plant and animal products, bio wastes, *etc*. Hence, the structure and chemical composition of CDs are complex and vary with the different precursors, solvents and post-treatment methods used. A natural precursor contains several active ingredients, and sometimes with unknown composition upon subjecting to different reaction conditions produces complex carbonaceous nanoparticles and byproducts with non-uniform chemical compositions, which can also contribute to fluorescence.[40–44] Moreover, the use of dopants generates CDs with diverse surface functional groups that possess their own definitive PL mechanism. Consequently, a unified explanation for the origin of fluorescence is yet to be reported.

Presently, three main perspectives are proposed for the fluorescence emission of CDs: (i) quantum captivity or core-state/size-dependent emission, induced by perfect carbon crystals with modified groups and fewer defects, (ii) surface-state emission based on the hybridization of the carbon framework and associated functional moieties and (iii) molecular fluorescence due to free or bound fluorescent impurities formed from the byproducts during the synthesis of CDs.[45,46]

Core emission (quantum confinement effect or size-dependent emission)

It is well-established that the emission behavior of a material having the size of a Bohr radius (<10 nm) is governed by quantum confinement, and therefore displays unique PL properties.[47] The PL peaks are narrow and excitation independent with a definite size-dependent emission property. The crystalline carbon core of CDs in the nanometer scale size significantly influences the electron distribution, resulting in bandgap- and size-dependent energy relaxation dynamics, consequently affecting the emission phenomenon.[48,49]

Kim *et al*. concluded that the red-shifted emission behavior of CDs is associated with the increase in the nanoparticle size and tentatively suggested that the fluorescence is because of the quantum confinement effect.[49] Furthermore, Li *et al*. also demonstrated that the fluorescence of CDs arises from the quantum confinement effects and is size-dependent.[11] In the meantime, Sun *et al*. attributed the fluorescence emission from CDs to the presence of surface energy traps that became emissive upon surface passivation due to their quantum confinement effect.[47] Yuan *et al*. synthesized CDs with multi-colour emission by using a nitrogen (N)-rich source under solvothermal conditions. The bandgap (3.02 to 2.12 eV) dependent emission was confirmed *via* transmission electron microscope (TEM) imaging, wherein the CDs with average size distributions of 1.95, 2.41, 3.78, 4.90 and 6.68 nm displayed corresponding blue, green, yellow, orange, and red fluorescence.[50] The bandgap-dependent emission was also proved through lifetime measurement to display a mono-exponential decay nature for all CDs with the QY estimated as 75%, 73%, 58%, 53%, and 12%, respectively. Another research group synthesized size-dependent emissive CDs from citric acid and urea by employing different solvent systems including water (CDw: 1.7 nm), glycerol (CDg: 2.8 nm size) and DMF (CDd: 4.5 nm size).[51] They proposed the full color emission mechanism for the CDs based on the extent of graphitization of the carbon core, suggesting a higher degree of dehydration and graphitization of CDs upon using aprotic solvents, resulting in a greater proportion of sp^2 than sp^3 carbon (Fig. 2a). In yet another report, multi-colour emissive CDs were prepared through solvothermal synthesis by varying the composition of the precursors. Blue and green (3.6 nm size) emitting CDs were obtained from *m*-phenylenediamine, whereas yellow and red emissive CDs (4.8 nm size) were produced from the same source in the presence of tartaric acid, which suggested that size plays a critical role in the characteristic emission behavior.[52]

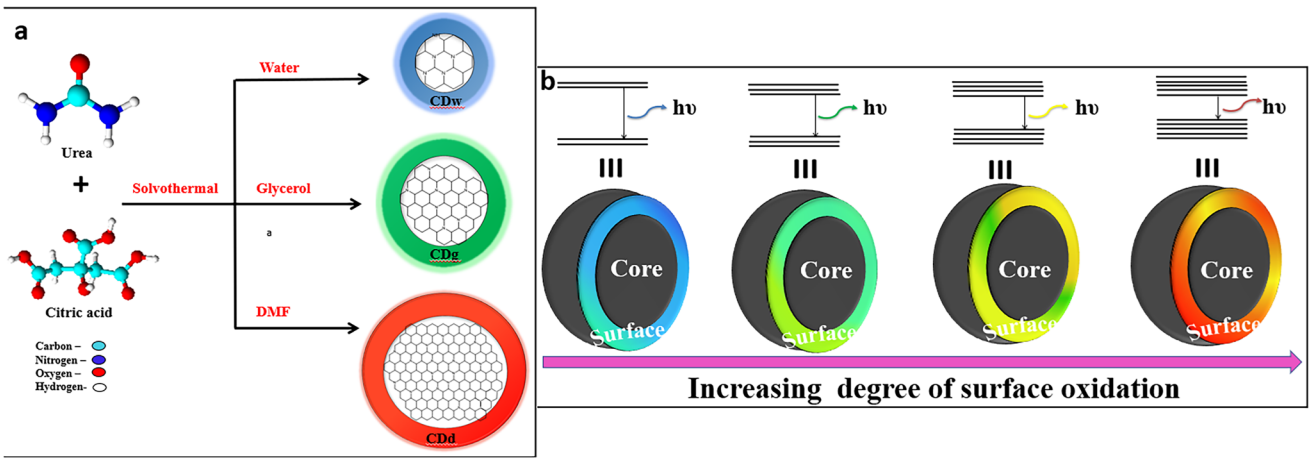

Fig. 2 (a) Full-color fluorescent CDs depicting size-dependent emission[51] and (b) full-color luminescent CDs with a surface-state-controlled emission.[57]

Surface state of CDs

The surface state including diverse functional groups and degree of surface oxidation serves as energy-trapping sites and is intently linked to the emission of CDs, which is one of the most widely accepted mechanisms for fluorescence. Light of a specific wavelength corresponding to the bandgap of the CDs induces excitation of electrons to a higher energy level, which upon relaxation are trapped on the surface defective sites. Later, when they return to the ground state, the energy difference falls in the visible region, shifting the emission to a longer wavelength range.[53] Wang *et al*. demonstrated the effect of surface functionalities on the emission centers of the CDs.[54] Liang's group reported N-doped CDs having same oxygen content with tunable multicolor fluorescence from dark blue to red or even white that originated from the surface functional groups.[55] The return of electrons in the N-related defect states to the highest occupied molecular orbital (HOMO) causes a red-shifted emission.

A few reports suggest that as the degree of surface oxidation increases, the amount of surface defects also rises, these serving as exciton capture centers leading to a red-shifted emission in the CDs.[56] Xiong and team obtained CDs purified through column chromatography, which showed excitation-independent emission from blue to red.[57] The band gap reduced with increasing surface oxygen content to showcase the red-shifted fluorescence. Liu *et al*. prepared green-emissive CNDs and yellow-emissive GQDs with a similar size distribution as well as chemical groups, but showed a bathochromic shift in the emission due to different degrees of surface oxidation.[58] This observation is because of the decreased band gaps between the lowest unoccupied molecular orbital (LUMO) and the HOMO. The reports by various groups including Zhu *et al*. and Ding *et al*. also proved that the oxygen-related surface states are responsible for the red-shifts in the emission of CDs obtained by hydrothermal treatment and subsequent purification using column chromatography[57,59] (Fig. 2b). Similar observations were reported wherein diverse surface states were introduced on CDs either by a controlled pyrolysis temperature or different combination of dopants. Miao and team developed B-CDs (3.96 nm size, λ_{em} = 440 nm, QY = 52.6%), G-CDs (4.12 nm size, λ_{em} = 540 nm, QY = 35.1%) and R-CDs (4.34 nm size, λ_{em} = 600 nm, QY = 12.9%,) indicating that size-dependent emission cannot be used to relate to the PL of the CDs.[60] However, surface state-induced emissions can explicitly explain the introduction of a cocktail of chemical groups, with increased oxygen groups in R-CDs in comparison with G-CDs and B-CDs.

Core emission and surface state of CDs: synergistic effect

A few pieces of evidence suggest the involvement of both the quantum confinement effect and the surface state in the fluorescence emission of CDs.[60,61] Pang and research group demonstrated that the fluorescence originates from the surface state emission, wherein the surface properties, the π-electron system and the size of the CDs determine the surface state energy gaps.[62] The increase in the amount of surface oxidation or particle size results in a red-shifted emission of CDs. Huang and group proposed that the confinement effect and the surface state synergistically affect the CD emission.[63] They also demonstrated that the carbon core size can be adjusted, and the surface functional groups of the shell can be manipulated to tune the fluorescence properties of the CDs.

Molecular fluorophores

During the formation of CDs, fluorescent impurities or molecular fluorophores are also generated. The presence of these fluorescent impurities, either attached to the CD surface or found freely floating in the as-prepared sample solution, is inevitable and contributes to the emissions of CDs with reportedly higher QY values, but the emission intensity diminishes over time as they are prone to photobleaching.[64,65] Although several mechanisms are hypothesized, the molecular fluorophores differ majorly with the precursor and the reaction conditions. Krysmann *et al*. synthesized carbon nanoparticles at 180, 230, 300 and 400 °C and compared their PL properties.[66] The QY measured for CDs corresponding to 230 °C (15%) is less in comparison with that obtained at 180 °C (50%), which indicates the predominance of molecular fluorophores at a lower temperature and moreover, with a gradual increase in temperature the carbonaceous core is developed at the expense of these fluorogenic particles (Fig. 3a).

To identify the chemical composition of molecular luminophores, nuclear magnetic resonance (NMR) spectroscopy coupled with mass spectrometry (MS) is performed. Duan *et al*. demonstrated a high fluorescence QY of CDs prepared from citric acid and ethylenediamine.[67] However, they proved that the as-prepared mixture contains imidazo[1,2-*a*]pyridine-7-carboxylic acid (IPCA), isopropyl chloroacetate, polymers and carbon cores, wherein isopropyl chloroacetate contributes to the intense blue fluorescence and high QY. Similarly, Rogach's and Baker's groups proposed that the molecular fluorophores attached to the CDs contribute distinctly to the optical features of the CDs.[68,69] Furthermore, Righetto *et al*. established that small emitters in the excitation range from 320 to 450 nm that are dispersed in solution contribute to the fluorescence of CDs,[70] whereas weak fluorescence observed above 480 nm excitation is majorly due to the poor-emitting carbon cores. Therefore, although carbon cores exist, the fluorescence origin is dominated by small organic molecules that are free in solution.

Zhang and team identified two fluorophores, 5-oxo-3,5-dihydro-2*H*-thiazolo[3,2-*a*]pyridine-7-carboxylic acid (TPCA) and 5-oxo-3,5-dihydro-2*H*-thiazolo[3,2-*a*]pyridine-3,7-dicarboxylic acid (TPDCA), which were found to display similar emission behavior to the CDs (Fig. 3b).[71] Besides, the QY of TPCA (66%) and TPDCA (76%) was closer to the QY of the CDs (64%). The contribution of these fluorophores was evaluated further by subjecting them to dialysis (1 kDa) wherein the dia-

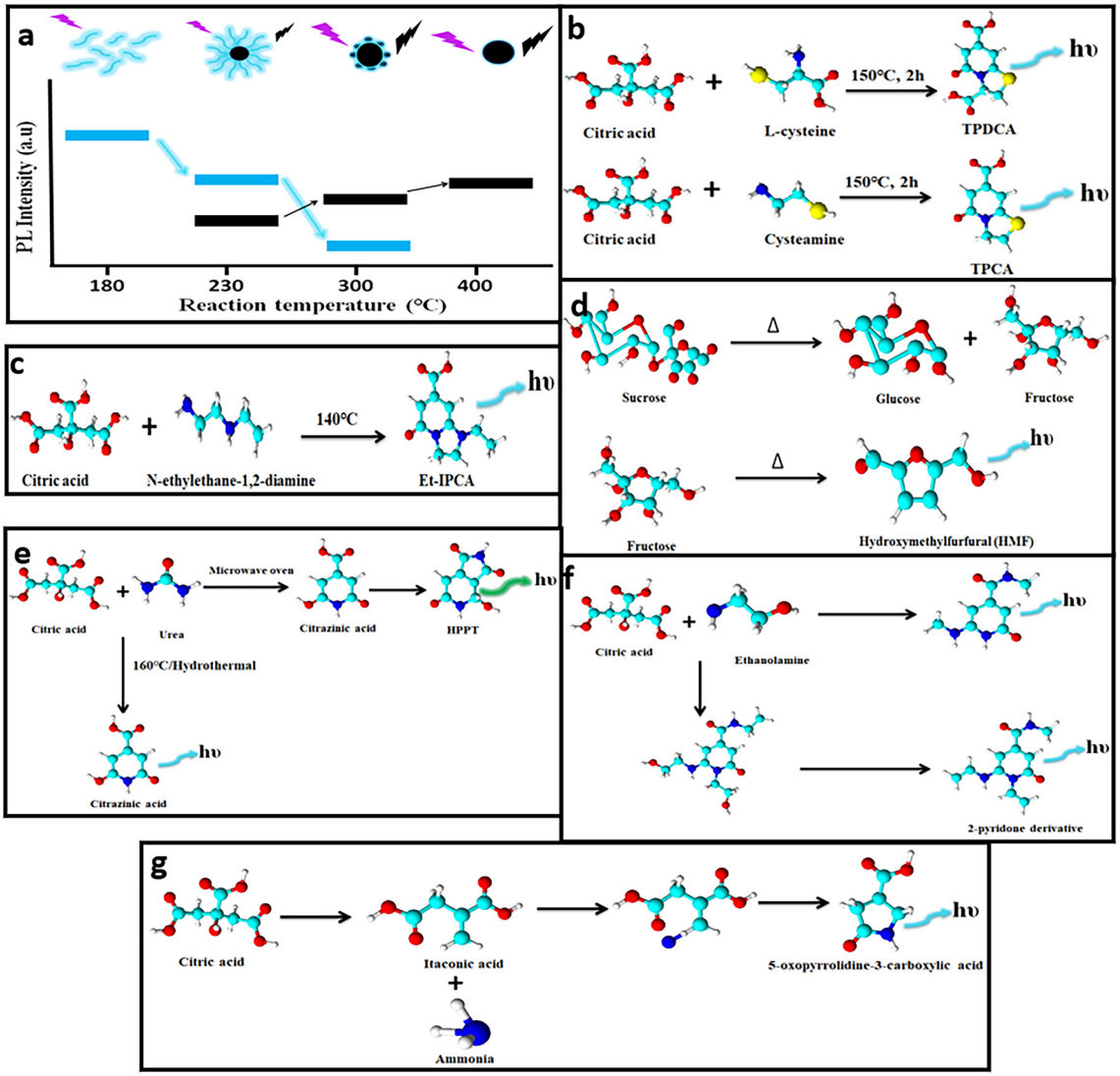

Fig. 3 (a) Emission intensity of CDs using citric acid and ethylenediamine as precursors during synthesis under different temperatures.[66] (b–f) Different types of molecular fluorophoric species[71,73–76] and (g) unconventional aliphatic fluorophores identified that contribute to the fluorescence of CDs.[77]

lysate demonstrated a higher QY in comparison with the residual retentate solution. Both the solutions exhibited similar emission attributes indicating the presence of these fluorophores. In addition, both the solutions were exposed to a UV source, which displayed nearly no fluorescence as these fluorophores are more prone to photobleaching.[71] Several fluorophores including IPCA, 5-(hydroxymethyl)furfural (HMF), 4-hydroxy-1*H*-pyrrolo[3,4-*c*]pyridine-1,3,6(2*H*,5*H*)-trione (HPPT), citrazinic acid, and a 2-pyridone derivative (Fig. 3c–f) were identified and separated, which induced fluorescence increments in CDs.[72–76] To date reports show the formation of fluorophores with aromatic structures but recently, a new kind of fluorophore was identified by Yao *et al.*[77] The blue-emissive fluorophore was produced during the synthesis of CDs using urea and citric acid (Fig. 3g). The hydrothermal product was dialyzed and subjected to reversed-phase column chromatography to obtain various fluorophore fractions. The NMR analysis showed numerous peaks in the aliphatic region. In a separate experiment, itaconic acid was prepared when citric acid undergoes dehydration and decarboxylation, and further subjected to hydrothermal treatment after adding urea. The raw product obtained possessed similar NMR spectroscopy and electron spray ionisation-MS spectra to the dialysate obtained from citric acid and urea. Hence, it was established that the new fluorophore was 5-oxopyrrolidine-3-carboxylic acid and possessed similar emission properties to itaconic acid. Thus, it can be concluded that fluorophores are the main species that induce changes in the fluorescence of CDs and their identification is possible by efficient separation and characterization *via* NMR and MS techniques.

Significance of purification and characterization of CDs

The presence of small molecular weight or oligomeric luminescent impurities and byproducts that result from incomplete reaction of the precursor contributes mostly to the emission of CDs and may strongly affect the optical properties, which demands the inevitable need to purify the synthesized products. Elucidating the true nature of these emergent nanocarbonaceous materials is of vital importance as inadequate purification poses a primary setback in their versatile applicability. Moreover, the complexity increases when plant/animal-based precursors are used, and their chemical composition remains unknown. Fluorescent impurities that originate during synthesis create an enormous obstacle to the analysis of the PL properties of CDs. They can change or even mask the actual optical features of the CDs to show dramatic differences in the fluorescence performances.[78] The molecular fluorophores that are present along with CDs contribute to most of the PL emission, suggesting towards their removal for reliable fluorescence results that originate only from the homogeneous CDs. Bartolomei and Prato briefly discussed the importance of purification and chemical analysis to identify the molecular fluorophores.[79] Therefore, the role of purification is imperative to separate the CDs from the constituting byproducts to rule out the possible errors associated with interference by these fluorophores.

Bottom-up methods are extensively utilized for CD synthesis due to their easy synthetic protocol and wide choice of precursors. The high temperatures involved results in not only the carbonization of the precursor, but also yield small molecular weight luminophores. Though various purification techniques are utilized to separate the fluorescent CDs from the remnant fluorescent byproducts, the extent of purification is unknown and challenging to prove.[69,80] Though TEM and atomic force microscope (AFM) imaging enable us to view the CDs with definitive lattice *d*-space values, the presence of molecular fluorophores cannot be examined. Therefore, inaccurate understanding is gained with respect to the purification of the small carbonaceous luminophores. The PL emission as well as QY measured for the purified sample is interpreted as the inherent emission from CDs alone.[81,82] The most definitive and effective characterization technique to confirm the presence of CDs is NMR spectroscopy.[67] Bartolomei *et al*. emphasize the necessity to incorporate NMR spectroscopy as a standard and an essential tool to minimize the risk in analyzing the fluorescence that originates from residual molecular species in the final sample, rather than the target CDs.[83] It can unveil the occurrence of molecular species in a rapid and easy-to-operate approach. The chemical shift peaks for the nanocarbons appear as broad and unresolved due to their complex chemical environment. In contrast, the appearance of sharp and resolved peaks is indicative of the presence of small molecules with specific groups.[67]

Despite the purification techniques adopted, these luminophores are not eliminated due to non-optimization of the purification procedure. For instance, Essner *et al*. pointed out the importance of the usage of appropriate molecular weight cut-off (MWCO) dialysis bags, as the smaller dimension can hinder the flux of CDs.[69] Yang and group reported the formation of small fluorophores during the synthesis of CDs using citric acid at lower temperatures, and upon a gradual increase in temperature the carbon cores are formed at the expense of these fluorophores.[72] They also proved that the CDs were composed of IPCA, polymer and a carbonaceous core which contributed to the blue fluorescence. Moreover, they identified IPCA as one of the fluorophores, which is highly emissive and obtained after column chromatography separation. The fluorophore was prepared separately while the same fluorophore was separated from the CDs *via* column chromatography and confirmed *via* NMR spectroscopy. Based on these findings the PL mechanism and structural relationship between the fluorophore and CDs could be elucidated; the excitation-independent emission and high QY were mainly due to the presence of the IPCA moiety.

When small molecules like sucrose, glucose and fructose are subjected to hydrothermal treatment, CDs are formed along with HMF derivatives as the condensation product. Gude *et al*. identified these fluorophores after solvent extraction and column chromatography separation of the synthesized product.[74] However, the NMR spectrum of the purified CDs matched with the NMR spectrum of the HMF except for the presence of an aldehyde group instead of a hydroxyl group. Additional confirmation is obtained *via* MS analysis where the *m*/*z* peak corresponds to the HMF dimer in agreement with the molecular weight of the HMF derivative. Besides, they display mono-exponential decay along with excitation-independent emission indicating that the CDs are composed of aggregates of HMF. The same research group prepared CDs from citric acid and ethanolamine and purified *via* a column chromatography method using a suitable elution system.[76] It was confirmed *via* NMR and MS analysis that the fluorophore obtained is a 2-pyridone derivative. Furthermore, the single-particle spectroscopy suggested otherwise that CDs constitute aggregates of fluorophore due to a gradual decay with respect to time along with greater photostability. Kasprzyk and team attempted to associate the blue and green emissions of CDs to the molecular fluorophore generated during the synthesis process. The product sample was purified *via* a high-resolution liquid chromatography electron spray ionization MS method enabling the efficient separation of different fractions. The blue emission observed was due to the formation of citrazinic acid as a condensation product, which converts to green-emissive HPPT when subjected to a dehydration step.[75] Bartolomei *et al*. demonstrated the importance of NMR spectroscopy to differentiate chiral emissive CDs from emissive molecular species by performing dialysis and high-performance liquid chromatography (HPLC).[83] These demonstrative studies highlight the importance of optimizing the purification protocol for the reaction mixture obtained after the synthesis of carbonaceous nanomaterials. In addition, the role of NMR and mass spectra evaluation as effective character-

ization tools to identify the different kinds of fluorophore generated during the synthesis of carbon dots is also evident.

Though numerous studies on CDs briefly explain the different purification procedures adopted in various research investigations, their impact on the fluorescence properties is not reviewed in detail. This unveils the need for a critical and concise appraisal of the use of appropriate purification techniques and their optimization to obtain reproducible and consistent fluorescence features from the CDs. The different purification techniques and their intricacies involved are briefly discussed.

Purification and separation methods for CDs

It is to be noted that a universal method for the purification and separation of CDs does not exist, but specific protocols can be established according to the nature of the products obtained after the synthesis procedure. The following section attempts to summarize the different techniques reported (Fig. 4) by various research groups to separate the CDs from other reaction products and provides a comprehensive understanding of the extent of purification attempted to separate the nanocarbonaceous material.

Filtration

Filtration is a simple method of purification where the as-synthesized CD product comprising different-sized nanoparticles is allowed to pass through filters of fixed pore sizes. The larger particles that are unable to penetrate the pore remain on the filter surface while the smaller particles are obtained as filtrate. This method can serve as a preliminary purification step to separate the insoluble or suspended particles or agglomerates in the CD sample obtained after synthesis. However, the pore diameter of the filter ranging between 0.1–1 μm needs to be optimised as there is tendency to clogging of the pores. Moreover, the concentrated sample needs dilution prior to filtration to avoid clogging. Previous reports on the purification of CDs state either the use of filters with definite pore sizes or the use of syringe filters. Sun *et al.* synthesized CDs from human hair fiber *via* heat-assisted sonication, wherein the remaining strands of hair were separated from the product utilizing a porous membrane of 0.22 μm pore diameter.[84] Lan *et al.* prepared carbon nanoparticles from melamine and trisodium citrate dehydrate and the resultant product was purified using a 0.22 μm pore size membrane.[85] Another study reported the synthesis of CDs using chitosan and ethylenediamine as precursors by microwave-assisted heating to induce dehydration.[86] The resultant powder was re-dissolved in water and filtered utilizing a syringe filter of 0.45 μm dimension to eliminate dissolved salts and unreacted chitosan. Although filtration is a less time-consuming approach for purification, the product requires additional purification as the separation does not isolate specific-sized particles.

Centrifugation

Centrifugation is yet another simple and inexpensive technique used in the initial purification to segregate small sized

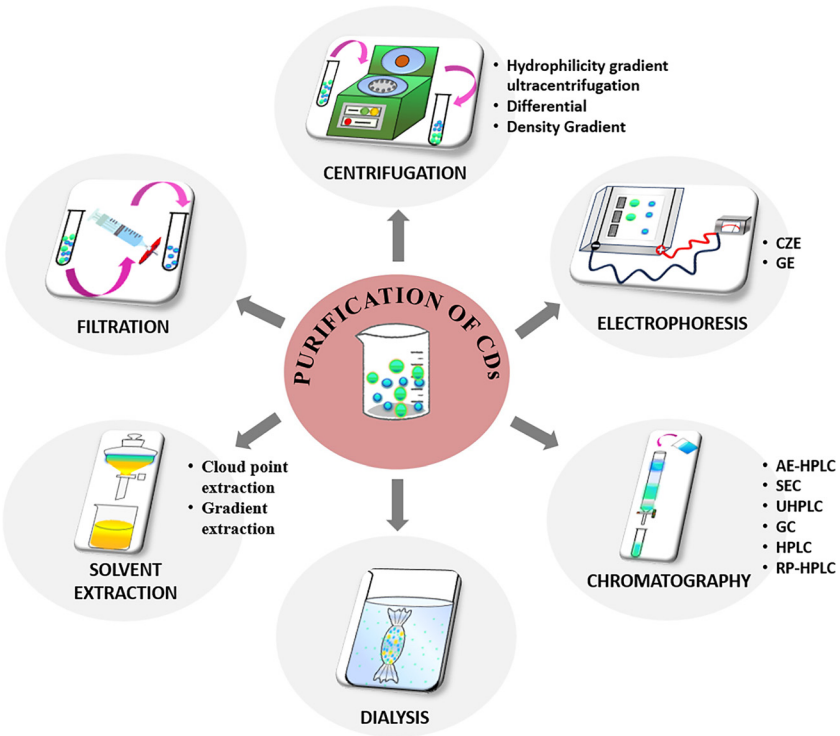

Fig. 4 Different techniques reported for the purification and separation of CDs.

carbonaceous nanoparticles from large aggregates or suspended particles from the product.

Density gradient centrifugation. It involves the separation of CDs based on density and mass wherein the precipitate, aggregates and larger particles settle down as sediment. The supernatant for further analysis comprises smaller particles having a significant density difference in comparison with the sediments which are separated. During centrifugation, the sample is subjected to a centrifugal speed ranging between 8000–13 000 rpm for a few minutes. Briefly, the sample is added on the top of a density gradient established by solutions of different densities layered sequentially. Upon centrifugation, the particles deposit in the density gradient at distinct speeds based on their shapes, sizes, or densities and ultimately form diverse bands. Several literature reports mention the use of centrifugation employing different radial speeds to remove the less-fluorescent and insoluble particles, while the highly fluorescent supernatant is collected for further purification.[87–92] The advantage of centrifugation is that both organic/aqueous soluble constituents can be separated to collect concentrated samples.

Sucrose, glycerol, cesium chloride, and other aqueous solutions are usually used to prepare the density gradient. Sucrose density gradient centrifugation (SDGC) enables the isolation of the nanodots of desired size and shape by varying the sucrose concentrations in the gradient for diverse applications, especially biological. Pandey *et al.* reported the fabrication of crystalline CDs from highly alkaline sugar cane juice at 28 °C and the separation from amorphous carbonaceous materials using the lucid and non-toxic SDGC technique.[93] A gradient was achieved in the test tube by overlaying 50–100% of pure sucrose, commencing from the highest concentration at the bottom. About 2 mL of the sample to be fractionated was top-layered and spun at 6000 rpm for 30 min. Fine separation was accomplished based on nanoparticle size due to the sharp density gradients (Fig. 5a).

Differential centrifugation. This separation approach relies on the isolation of multiple fractions within a CD sample based on size and density through a stepwise increase in the centrifugation forces. At lower centrifugal speeds, the larger and denser particles precipitate whereas the smaller and lighter particles stay in the supernatant and need more centrifugation as well as force to settle down.[94] The CD sample mixture is centrifuged multiple times, and the precipitate is removed after each run. Furthermore, the supernatant is centrifuged at a higher centrifugal force. Sahu *et al.* reported the hydrothermal treatment of orange juice and obtained different size-range CD species through a differential centrifugation method.[95] During the separation process, the brown aqueous CD solution was centrifuged at 3000 rpm for 15 min initially to deposit the less-fluorescent coarse nanoparticles (30–50 nm size). Subsequently, the brown CD solution was centrifuged at a higher speed of 10 000 rpm for 15 min after adding excess acetone to obtain highly fluorescent CDs (1.5–4.5 nm size) in the supernatant (Fig. 5b).

Hydrophilicity gradient ultracentrifugation. The separation based on the differences in colloidal stability or solubility (varied hydrophilicity) of CDs in dissimilar media forms the basis of the hydrophilicity gradient ultracentrifugation method. This technique further broadens the sortable nano-

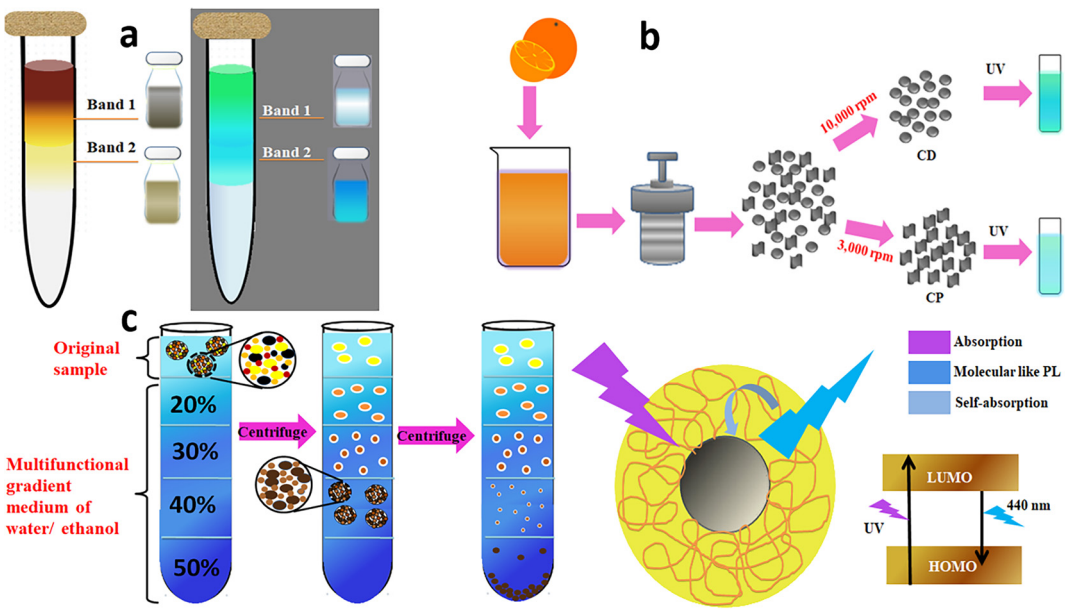

Fig. 5 (a) SDGC separation of CDs from the sonication of sugar cane juice and the separated CD bands under ambient and UV light,[93] (b) differential centrifugation of hydrothermally obtained orange juice-derived CDs to deposit the less-fluorescent coarse nanoparticles and highly fluorescent CDs.[95] (c) Hydrophilicity gradient ultracentrifugation wherein the CDs are clustered at the starting point and de-clustered at successive layers with increasing water content during sedimentation, and the proposed PL mechanism of the CDs.[96]

particle range. Deng *et al*. used a hydrophilicity-triggered grouping approach for the size sorting of non-sedimental CDs with different degrees of carbonization formed through the hydrothermal dehydration of ethylenediamine and citric acid.[96] Common ultracentrifugation failed here because of the immensely high colloidal stability of the CDs, and therefore these carbonaceous nanodots were forced to sediment through ethanol and water gradient media (a gradient of both hydrophilicity and density) with four volume ratios. Primary CDs having different sizes and carbonisation degrees dispersed in the respective gradient layers were achieved. The hydrophilicity and solubility of the environmental media determined the settling level. The PL of the CDs originated mainly from the radiative recombination of excitons associated with their surface molecular state rather than the quantum size effects of the carbonised cores (Fig. 5c).

Dialysis

Dialysis is one of the purification techniques used extensively to remove low molecular weight residual precursors and polymers to separate the CDs. Water-soluble CD samples can be easily filtered and dialyzed. The process relies on the diffusion of small fluorescent molecules from a higher concentration region to a lower concentration area across a semipermeable membrane. During this process, the as-synthesized CDs are dissolved in deionised water and dialyzed with stirring against an appropriate MWCO dialysis bag (semipermeable membrane) in deionised water. Gradually, the low molecular weight components diffuse out due to the concentration gradient and constitute the dialysate, while the remnant solution inside the bag called the retentate comprises high molecular weight species. The constituent of the dialysate depends upon the sample concentration, duration and MWCO of the dialysis bag. Maintenance of the sample pH is tedious, and the buffer solution must be recharged or changed periodically with fresh deionised water at various time intervals to hold the dialysate dilute.[97] The MWCO of the dialysis membrane, the stepwise process in terms of water replacement and the duration of dialysis require suitable optimization to realize the best purification outcome. Though hydrophobic samples cannot be separated *via* this technique, dialysis is employed extensively as one of the purification techniques in several research studies.[69]

Kang and group synthesized blue-emissive CDs from PEG *via* a hydrothermal approach. The dark-coloured sample was subjected to dialysis (MWCO 1 kDa) until the solution changed to golden yellow (Fig. 6a) to provide the initial indication of the completion of purification of the CDs.[98] Similarly, Liu *et al*. synthesized CDs from PEG and NaOH and the resultant brown solution was dialyzed (MWCO 1 kDa) until a clear golden solution was obtained.[99] Yet another research group used a similar MWCO dialysis bag to obtain hydrophilic and blue-emissive CDs. The dialysis was carried out for 3 days to completely remove the molecular precursor. Despite the

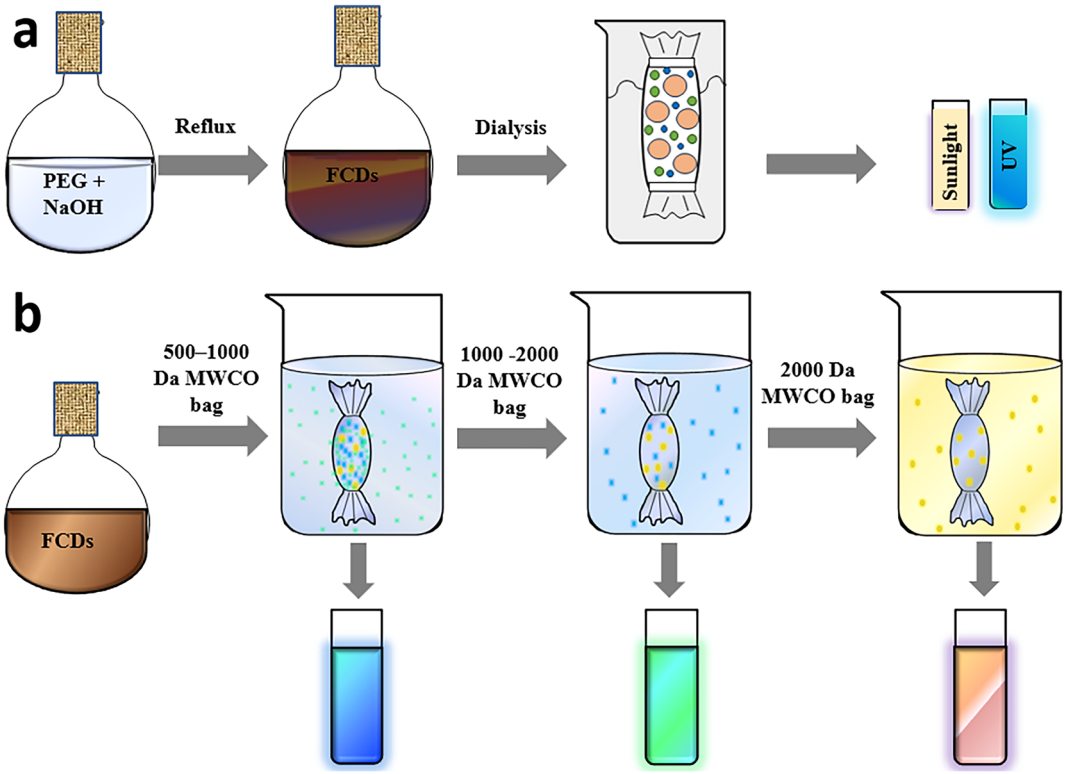

Fig. 6 (a) Simple dialysis for the purification of PEG-derived CDs,[98] (b) concentrated dialysate obtained for 500–2000 Da dialysis bags and illustration of samples when exposed to 365 nm UV irradiation.[108]

extensive purification carried out, the CDs displayed a QY of 2.03%, 10.28%, 19.72%, and 27.66% corresponding to a pyrolysis period of 1, 2, 3 and 4 h respectively. Besides, TEM analysis confirmed the presence of small and narrow-distribution-sized CDs.[100]

Most studies report the dialysis of CDs using a low MWCO of 1 kDa, performed with the intention of separating only the smaller sized CDs from the remnant precursor and byproducts.[59,101–104] Therefore, an attempt was made by Yuan *et al*.[105] and Feng *et al*.[106] to use dialysis bags of MWCO of 3.5 kDa. The TEM images of the CDs present in the dialysate depicted a narrow distribution indicating successful separation and optimisation of the dialysis procedure. Noun and team reported that the initial dialysate of the CD sample had a lower QY, indicating the presence of less-emissive fluorophore.[107] However, upon further dialysis there was an increment in QY by many fold, suggesting that highly emissive fluorophores formed can be removed *via* an organic solvent wash, thereby reducing the QY. Thus, the dialysis process must be monitored at every stage *via* photophysical spectroscopic analysis to evaluate the accuracy of purification for a specific system.

Although the composition and population of fluorescent species formed along with CDs vary based on the precursor used and reaction conditions maintained, these highly fluorescent small-sized species can pass through the permeable dialysis membranes. Hence, the rationale behind choosing the appropriate MWCO is a matter of curiosity, inviting numerous trials to separate CDs as the sample has an unknown product composition. Zhang *et al*. used smaller (500 Da) to bigger dimension (2000 Da) dialysis bags (Fig. 6b) with the intention of separating the smaller fluorophores initially, and then the CDs.[108] After subsequent dialysis the decrease in QY of the retentate indicated that the small-dimension fluorophores are highly emissive in comparison with the CDs. Essner *et al*. used dialysis bags of different molecular weight; accordingly, the retentate from an MWCO of 1 kDa showed the presence of larger particles during TEM imaging, while dialysis with a 20 kDa membrane displayed a better separation of CDs.[69] Chang *et al*. reported a detailed investigation on the purification of citric acid-derived CDs using dialysis.[109] Dialysis was performed for different durations to completely remove the molecular luminophores and the retentate was analysed *via* HPLC coupled with fluorescence spectrophotometry. With time, the fluorescence QY of the sample inside the dialysis bag diminished from 2.2% to 0.6% and the retentate concentration declined from 580 to <1 mg mL^{-1}. This suggested that the sample solution is largely composed of small molecule byproducts and the actual CDs formed are very low. Besides, the UV–vis absorption and fluorescence peaks of both the retentate and dialysate obtained *via* HPLC demonstrated remnants of many byproducts in the retentate even after 24 h, suggesting ~72–120 h of dialysis is essential to eliminate the highly emissive molecular impurities from the CD solution. Besides, the use of MWCO <1 kDa was not necessary as most of the species were trapped within the dialysis bag. This study vividly highlights not only the significance of the purification of the CDs, but also stresses the necessity to customize the dialysis parameters according to the sample under investigation. In contrast, if nanocarbonaceous materials had better solubility in organic solvents, the residual impurities could have been removed through solvent extraction and/or precipitation.

Though these findings do not hold absolute claim, they encourage researchers to re-think about the impact of different-MWCO dialysis bags and the dialysis duration on the separation of nanoparticles. Furthermore, these dialysis parameters need to be suitably customized in accordance with the investigated sample to achieve a complete separation of CDs for further characterisation and practical application.

Solvent extraction

Liquid–liquid partitioning or solvent extraction has been widely utilised in the separation of CDs from the product mixtures after synthesis. This method is used when the precursor is hydrophobic, and dialysis cannot be employed. The sample consisting of hydrophobic/hydrophilic components can be separated based on its solubility in two immiscible solvents (an organic solvent and water), and the components distribute among the solvents. Chloroform, ethyl acetate, *n*-hexane, acetone, and toluene are the generally used solvents to extract the amphiphilic CDs and completely retain the impurities in aqueous solution.[110–112]

The disadvantage of this method is that although a separation of components in two or more immiscible liquids is obtained, each separated solution may contain more than one type of species. The validity of separation can be checked on TLC plates, which could suggest the presence of different compounds. Moreover, it is difficult to distinguish and purify the reactants from the products when both have the same solubility. Depending upon the solubility of the CDs obtained during the hydrothermal/solvothermal process, different solvent systems are used. Goncalves and research group synthesized CDs by laser ablation and concentrated them using ethyl acetate to eliminate the remaining unreactants.[110] In another report, CDs were synthesized from acrylic acid and 1,2-ethanediamine, and the further addition of glycidyl methacrylate induced polymerization.[113] The polymerised product was separated from the oily phase *via* the addition of water and the latter was given an *n*-hexane wash to remove the unreacted glycidyl methacrylate. Yu *et al*. used ascorbic acid to prepare blue-emissive CDs by a solvothermal approach to obtain a dark brown product and the organic byproducts were removed *via* dichloromethane extraction.[114] The water fraction was further dialysed to eliminate the impurities to obtain CDs as small as 3 nm in size. In another synthesis process, the precursor was subjected to carbonisation and the CDs were extracted using chloroform in the form of a brown dispersion. The remnants of the reactants were removed through a hexane wash. Another research group reported the microwave-mediated synthesis of CDs from resorcinol and H_2SO_4.[115,116] The product was provided with an *n*-butanol wash to remove the unreacted impurities, and the CDs were concentrated *via* double distilled water

extraction. The CDs separated *via* solvent extraction demonstrated better QY and excitation-independent emissions in comparison with those obtained through a dialysis process. This indicates that the solvent interactions with CDs can confer enhancement in the emissive behaviour.

Gradient extraction method. The new gradient extraction purification approach relies on the surface polarity of the CDs. Han *et al*. proposed this simple and economical method for separating cow milk-derived CDs synthesized through a hydrothermal method.[117] Four organic solvents with differing polarities, hexane (0.06), carbon tetrachloride (1.6), a mixture of carbon tetrachloride and dichloromethane (v/v = 3 : 2), and dichloromethane (3.4), were exploited for extraction to collect the CD fractions. The four fractions obtained exhibited dissimilar surface polarities due to the different polar surface functional groups and showed, hence, different surface polarity-dependent PL (Fig. 7a). Red-shifted PL peaks with greater excitation-dependency and a longer lifetime were observed with increasing surface polarity of the CDs. The increasing amount of auxochromes with increasing polarity leading to an internal energy transfer process was proposed to explain the distinct PL properties of each CD fraction. The study also showed that the organic solution dispersion process has no evident influence on the PL behaviour and originated entirely from the separated CDs itself.

Cloud point extraction. Beiraghi and Najibi-Gehraz described a green method for the purification and fractionation of CDs with oxygen-containing functional units obtained through the thermal pyrolysis of citric acid.[118] The reaction product was purified and further fractionated into two distinct CD species through a pH-controlled cloud point extraction technique using the nonionic surfactant, Triton X 114. The process of separation of the synthesized CDs from the precursors involved two steps: (i) the CDs were separated from polar impurities including unreacted citric acid or short-chain polymers generated during the synthesis, which were expelled from the micellar phase and persisted in the aqueous media, and (ii) the CDs were released from the micelles into the aqueous media upon changing the pH, while all the nonpolar impurities were entrapped within the micelles to realise a back-extraction (Fig. 7b). The extraction recoveries were increased with decreasing pH values. The surfactant molecules act as CD-conveyors, upon the formation and dissociation of micelles, which are 'filled with' and 'emptied out' of CDs, so that they can be used for repeated extraction processes. The CD extraction and fractionation is determined by the surface properties and the surface-density of oxygen-containing surface functional groups, particularly carboxyl and hydroxyl moieties, which plays a crucial role in their different pH-dependent behavior. The CDs tend to reside in the micellar phase at acidic pH when these groups are protonated, while the CDs show affinity towards the polar aqueous phase at a neutral or basic pH when these functional groups transform to their negative form. The separation method is considered as green because water is the only substance consumed during the extraction. The surface-chemistry of the separated fractions markedly influences the PL behavior of the CDs. CDs are assorted merely based on the abundance of hydrophilic surface functional groups, whereas the nanoparticle size does not play any determining role in the separation.

Chromatography techniques

The efficiency of separation of CDs is greatly enhanced when column chromatography is adopted. Chromatographic tech-

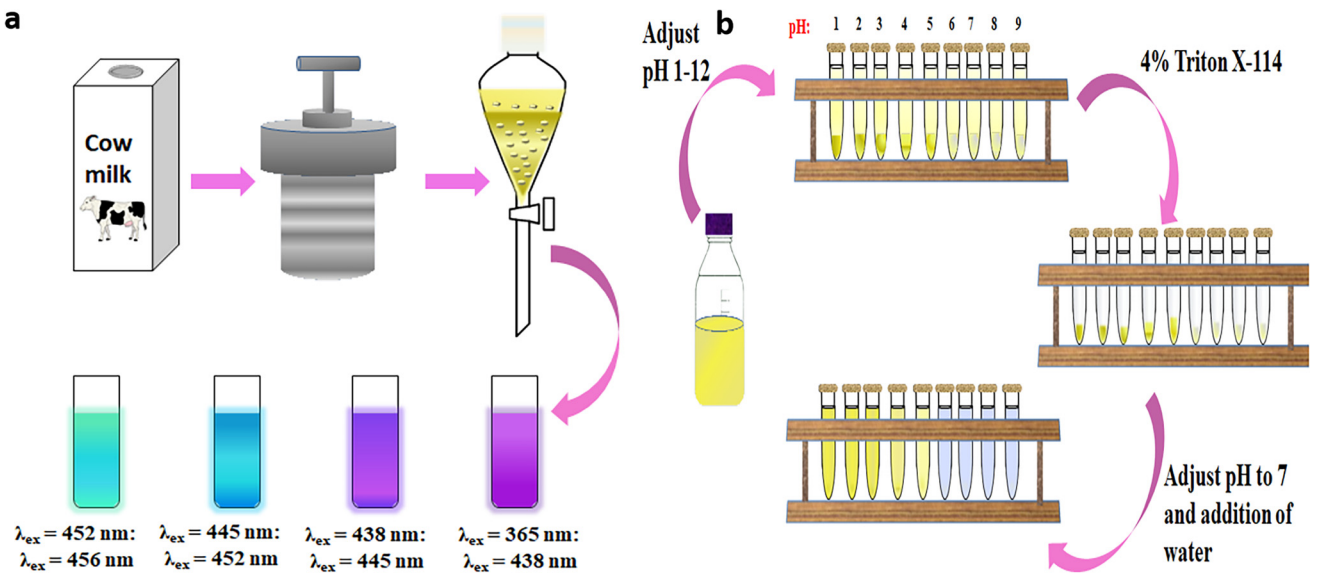

Fig. 7 (a) Schematic illustration of fabrication, gradient extraction, and surface polarity-dependent PL of isolated CDs,[117] and (b) cloud point extraction of CDs depicting the two phases separated during the first step of extraction, the separated micellar phase containing CDs and the second step of purification which returns the CDs to the aqueous phase.[118]

niques that are available for the separation of CDs include size exclusion chromatography (SEC), HPLC, anion-exchange high-performance liquid chromatography (AE-HPLC), reversed-phase high-performance liquid chromatography (RP-HPLC), and gravitational column chromatography.

Size exclusion or gel permeation chromatography. The as-synthesized CD mixtures are mostly composed of dissimilar-sized nanoparticles. SEC, with different amalgamations of solid and mobile phases, stands out as one of the most promising size-based separation methods. It includes both conventional low-pressure and high-performance techniques. SEC separation is achieved by the differences in the flow velocity within a column packed with porous stationary phase materials (Fig. 8a).[119] The smaller particles or those with equal size to that of the pores in the packing materials infuse deep into the column, leading to a longer retention time. However, larger particles that diffuse freely and move along with the mobile phase are excluded and are first to elute. Commercially available desalting columns are used for performing the size exclusion separation of CDs, and the sample is added to the top of the column and buffer or water is used as the eluting solvent.

It is well-established that the surface state plays a prime role in the fluorescence behaviour of CDs, resulting in size-independent emission. Wang *et al.* fractionated surface passivated (PEG1500N) fluorescent CDs through an aqueous column packed with Sephadex G-100 gel using water as the eluent to achieve CDs free of any non-fluorescent material for an enhanced QY close to 60%.[120] Jiang and team mixed Nescafe® coffee powder obtained *via* a hydrothermal method in distilled water at 90 °C and centrifuged it for 15 min at 14 000 rpm. The large or agglomerated particles in the supernatant were filtered off through a 0.22 μm membrane and the filtrate was loaded onto the Sephadex G-25 gel column with distilled water as eluent.[121] The isolated CDs displayed excitation-wavelength-dependent multiple emission colors, and fascinating up-conversion PL. Liu and team initially adopted dialysis to separate the precursor from the product and further obtained two fractions *via* a Sephadex gel column, which demonstrated characteristic emissions (Fig. 8b).[122] The PL pro-

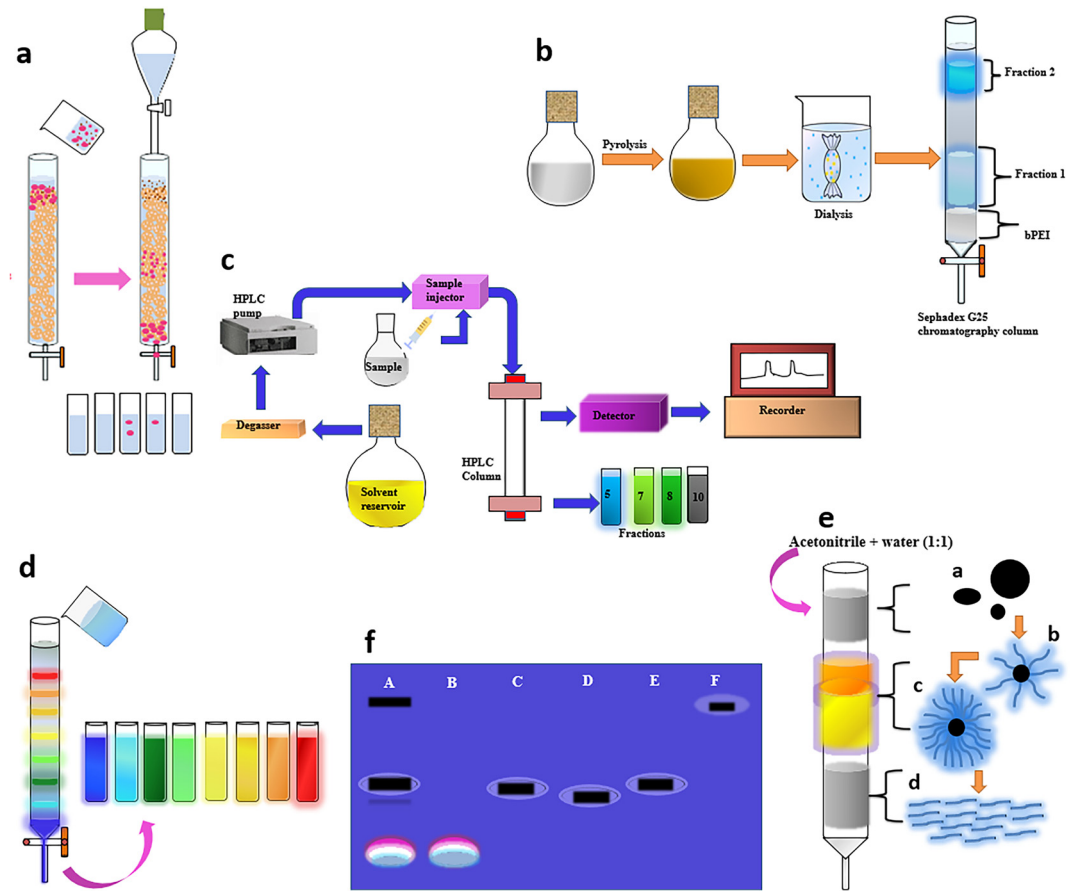

Fig. 8 (a) Schematic representation of particle size-based separation using SEC.[119] (b) Dialysis and subsequent SEC to obtain two CD fractions, which demonstrated characteristic emissions.[122] (c) Isolation of brighter CDs from an apparently low QY mixture using AE-HPLC[126] and (d) GC using a silica column to obtain a series of full-color light-emitting excitation-independent CDs with a surface-state-controlled luminescence mechanism.[57] (e) Purification of a citric acid and cysteine-derived CD mixture by GC to obtain three different fluorescent species.[131] (f) GE in a 1% agarose gel viewed under 365 nm UV light; A – crude suspension of single-walled carbon nanotubes suspension, B – fluorescent carbon, C – short tubular carbon, D and E – further separation of C, and F – cut single-walled carbon nanotubes.

perties were related to the surface passivation and not based on a quantum confinement effect. The second fraction with smaller particles that eluted last had a greater oxygen content and possessed a 17.4% QY in comparison with the first fraction containing slightly bigger sized CDs with a QY of 8.2%.

High-performance liquid chromatography. Fuyuno and team attempted to purify the CDs using HPLC and the separations were in accordance with the size exclusion principle.[123] Among the obtained fractions, the fourth, seventh and tenth fractions displayed distinct emission properties. The TEM imaging indicated size-based column chromatography separations. The PL plots for all the fractions displayed sharp peaks pointing towards the excitation-independent emission of CDs as opposed to a broad spectrum extending from the UV to the red region indicating the excitation-dependent property of the as-prepared CDs.

Ultra-high-performance liquid chromatography. The separation of neutral compounds can be done using ultra-high-performance liquid chromatography (UHPLC) as demonstrated by Gong *et al.*[124] The complex mixture of CDs derived through the microwave-assisted pyrolysis of chitosan and glacial acetic acid was separated using a UHPLC technique within 16 min. Among the 15 fractions, the initial fraction consists of CDs of multi-emissive sites, while the latter fractions are of greater purity. The PL spectra of 1–8 fractions displayed red-shifted emission with respect to the excitation but fractions 9–15 did not exhibit any changes in the emission bands.

Anion-exchange high-performance liquid chromatography. Generally, many CDs are reported to display a negatively charged surface. AE-HPLC facilitates the separation of negatively charged ions or molecules based on their affinity to the positively charged groups in the ion exchange resin. Vinci and Colon used AE-HPLC fractionation using an anion-exchange column and ammonium acetate as eluent to isolate the components from the complex mixture of soot-derived CDs produced during the flame-induced combustion of paraffin oil.[125] The CDs comprised species with different optical and electronic properties; the fraction that eluted out late displayed a longer PL wavelength. Later, the same group reported the use of a well-established high-resolution AE-HPLC method for the separation of CDs generated through the oxidation of graphite nanofiber.[126] They demonstrated that the fractionated samples did not exhibit wavelength-dependent PL, which is an inherent property of as-synthesized CDs. Moreover, the fractionated CDs exhibited profound differences in the fluorescence QY, allowing the isolation of brighter CDs from an apparently low QY mixture (Fig. 8c). Furthermore, the authors inspected the surface composition of the luminescent CD fractions using XPS and FTIR[127] and identified that the surface functionalities of all the carbonaceous nanoparticles were not identical, and they contributed differently to the observed PL. The CDs with intense fluorescence possess a lower oxygen content.

Reversed-phase high-performance liquid chromatography. RP-HPLC technique involves the high-resolution column separation of CDs wherein the mobile phase polarity is higher than that of the stationary phase. Gong *et al.* proposed the RP-HPLC method using a C18 column with methanol and Milli-Q water as the mobile phase to achieve the separation of chitosan-derived CDs synthesised by hydrothermal carbonization.[128] Initially, byproducts and low molecular mass species were removed using dialysis membranes with a small MWCO of 500–1000 Da. Further RP-HPLC was performed to obtain numerous nanospecies; the elution order followed from approximately small to large core sizes, to display unique optical and electronic properties as confirmed by UV-vis and PL spectroscopy. The emission peaks showed a slight bathochromic shift with an increase in relative molecular masses of the fractions. Later, Hu *et al.* coupled RP-HPLC with fluorescence detection for the fractionation of citric acid and 1,2-ethylenediamine derived CDs using methanol and 10 mM ammonium acetate (pH 4.5) as the mobile phase.[129] The size of the CDs increased with the elution order in RP-HPLC and displayed a red-shifted PL emission with increasing CD size. The fragmentation of the CD sample occurred in close relationship to the CDs' surface-attached COOH and $CONH_2$/NH_2 groups. The same research group reported the separation of a complex mixture of hollow CDs derived from acetic acid and P_2O_5 by an RP-HPLC method with a binary solvent mixture of 10 mM ammonium acetate buffer (pH 5.5) and methanol as the mobile phase.[130] The collected fractions displayed emissions spanning the red, green, and blue regions under 365 nm UV irradiation with good photostability.

Gravity chromatography. Gravitational chromatography (GC) is also utilised for the purification of CDs as mentioned in a few reports. Although it is a slow and time-consuming process, it is relatively simple and provides accurate separations on a par with much developed AE-HPLC techniques. Ding *et al.* purified a *p*-phenylenediamine and urea-derived solvothermal product by silica column chromatography to obtain a series of excitation independent CDs.[57] The different degrees of surface oxidation among the various fractions collected ultimately determined the fluorescence emission colors. The entire purification process took 10 h for completion due to its slow rate of separation. The eight eluted fractions (Fig. 8d) exhibited a characteristic emission when illuminated by UV light and a certain degree of red-shift in the emission for the more polar fraction. However, the TEM images showed that CDs possess the same size of 2.6 nm and lattice infringes with a *d*-space value of 0.21 nm. The surface passivation played a key role in determining the emission property. The red-emissive CDs have a greater proportion of oxygen content in comparison with the blue-emissive CDs. Hinterberger *et al.* synthesized CDs from citric acid and cysteine hydrothermally and purified the resultant product using a simple column chromatography unit and an isocratic elution system.[131] They demonstrated that the composition of the CD solution and the structure of the individual fluorescent components can be identified after chromatographic separation. The fractions having a low retention time that were the first to exit the column exhibited high fluorescence intensity and QY. Three different fluorescent species were identified; small organic byproducts and freely floating molecular fluorophores left the column first, followed by highly fluorescent CDs with fluorophores bound to the carbon

core, and lastly low-fluorescent carbon particles without fluorophores (Fig. 8e).

Electrophoresis

Electrophoresis is a method of purification performed in a conductive medium where the separation of particles takes place under an applied electric field. The migration of these particles is governed by the size, charge, and shape along with the prevailing temperature. This technique is cumbersome and can be employed when dialysis or column chromatography does not efficiently separate the particles. Moreover, it enables the physical segregation of positive and negatively charged particles. Electrophoretic separations of water-soluble CDs can be achieved through gel electrophoresis (GE) and capillary zone electrophoresis (CZE).

Gel electrophoresis. Different migration features by sieve effects under the influence of an electric field form the basis of the GE separation of CD samples. Xu *et al*. reported the polyacrylamide gel electrophoresis (PAGE) mediated separation of CDs when they were purifying single-walled carbon nanotubes derived from arc-discharge soot.[1] The electrophoresis of the sample in 20% denaturing gel (8 M urea, 1× TBE running buffer) performed at 55 °C by applying 600 V in an electrophoresis unit separated it into three types of nanomaterial: agglomerates that did not penetrate the gel, short tubular carbons as slow-moving dark bands, and fluorescent CDs as fast-moving multicolour bands (Fig. 8f). Liu *et al*. purified fluorescent CDs obtained through the oxidative treatment of candle soot using sodium dodecyl sulfate (SDS)-PAGE to obtain fast-moving and slow-moving bands along with agglomerates which did not penetrate the gel.[132] The initial bands displayed multi-colour fluorescence under excitation at 365 nm and the lower wavelength emissive CDs possessed a small size. In addition, the separations observed enabled the authors to conclude the relationship between a greater mobility of CDs with the emission color, wherein faster migrating CD species emitted at shorter wavelengths.

Kokorina and group utilised two-stage GE to study the constituent fragments of a CD sample obtained hydrothermally from ethylenediamine and citric acid.[133] The blue fluorescence with a higher QY confined to discrete bands that originates from the negatively charged small-sized light molecular fraction with the highest mobility and that shows no excitation-dependent light emission corresponds to IPCA. In contrast, bands having a lower QY, and displaying excitation-dependent emission are commonly observed for CDs with different emissive centres. Similarly, Sachdev and research group applied an SDS-PAGE method for the separation of polyethylene glycol and polyethyleneimine passivated CDs in a 12% denaturing gel under an electric field of 120 V.[134] Multicolour fluorescence was observed from the excised CD–polyethyleneimine band, whereas no fluorescence was visualised from the excised piece of CD–polyethylene glycol gel. The surface charge-dependent mobility of CDs was studied using GE in a 1.2% agarose gel run using Tris acetate–EDTA buffer under 85 V. Fluorescent bands of positively charged CDs–polyethyleneimine and negatively charged CDs–polyethylene glycol that migrated towards the negative and positive terminal, respectively, were visualised under UV illumination. PAGE can identify the correlation between the mobility and color of the fluorescent CDs. However, it has a low separation efficiency due to the ~3–5 nm pore size of the gel, which restricts its application in the separation of CDs with a wide size range.

Capillary zone electrophoresis. CZE is a useful separation approach wherein the CD solution mixture with components having different electrophoretic mobilities moves through an electrolyte solution contained in a fused silica capillary under the influence of an electric field. The separation occurs based on their charge/size ratio. CZE was coupled with a diode array detector by Baker and Colón to separate CDs obtained through the oxidation of soot from an oil lamp flame.[135] The study established the effect of the buffer composition on the electrophoretic pattern of a mixture of negatively charged CDs.

Though CZE is a simple, but powerful technique to realize an acceptable separation efficiency, the benefits offered by the high number of theoretical plates are dominated by the low sensitivity of the UV detection systems due to the small sample injection volumes.[136] To overcome this limitation, Hu *et al*. used a commercial CZE apparatus in combination with a diode array and laser-induced fluorescence detectors to separate and identify the composition of 1,2-ethylenediamine and citric acid-derived CDs synthesized *via* microwave-assisted pyrolysis.[137] The separation was achieved using a 40 cm capillary at an applied voltage of 15 kV with 30 mM sodium acetate–acetic acid as the run buffer of pH 3.6. The CZE technique was also effectively used to investigate the reaction time-associated kinetics of CD formation and identify the functional group-associated neutral, positive, or negative charge states, which influences the emission features. Wu and Remcho reported CZE coupled with UV absorbance detection for the rapid and reliable analysis of CDs using an alkaline working buffer of 100 mM Tris acetate at pH 8.4.[138] Table 1 highlights the different purification techniques adopted by researchers for the separation of CDs from various sources for diverse applications, along with their benefits and limitations.

Limitations and future perspectives

The facile synthesis of CDs through various physicochemical strategies from different carbon-based sources to realise desirable PL properties has led to a significant rise in the publications in various fields. However, the composition of as-synthesized CD samples, especially those formed through bottom-up chemical synthesis involving molecular precursors, is highly complex as they exist as mixtures of several CD fractions along with other molecular intermediates and side products with significantly different properties. Presently, no specific techniques are developed to certify the exact composition of these CD mixtures, which significantly complicates their targeted applications. The heterogeneous constitution hampers the explicit analysis of the CD sample for practical application as it can only represent the average features of the individual

Table 1 Analytical separation techniques adopted for CDs

Purification method	Separation device	Separation principle	Advantages	Challenges	Analytical applications
Filtration	Syringe filter	Filter with fixed pore size allows passage of smaller particles	• Simple and less expensive • Separation of large agglomerates from CD solution	• Though separation is selective, unable to separate fluorophores completely • Tendency to clogging of filter pores	Cell viability assay, Hg^{2+} & mercaptothiol sensing
Density gradient centrifugation	Tubular centrifuge	Separation based on density gradient	• Simple and inexpensive method to separate CDs from larger particles • Fine separation can be achieved • Separation of CDs both in organic and aqueous phase	• Low molecular weight fluorophores and precursors may not be separated from CD solution	Bioimaging of RBCs, *in vitro* imaging & fluorescent labels
Differential centrifugation	Centrifuge	Separation based on size and density	• Multiple fractions within a CD sample can be separated	• Mixture needs to be centrifuged multiple times	Cellular imaging
Hydrophilicity gradient ultracentrifugation	Centrifuge	Separation based on hydrophilicity and solubility of the environmental media	• Efficient approach for the separation of non-sedimental species with extremely high colloidal stability	• Proper choice of solvent system and optimisation of their volume ratios to realise the suitable gradient medium	—
Dialysis	Dialysis bags with different MWCOs	Permeable membrane with specific MWCO allows passage of CDs with specific size	• Can remove precursor species from CD solution • Can separate CDs of uniform size based on specific MWCO • Low molecular weight flurophores can easily diffuse out from dialysis bag	• Time-consuming, tedious, and expensive • Process often affected by solvents • Appropriate bag selection is crucial • Process duration needs optimisation • Cannot remove hydrophobic components present along with CDs • Requires HPLC to monitor the separated fluorophores • Dialysed sample gets diluted and needs to be concentrated for further experiments • CDs with dissimilar sizes or surface functional groups cannot be separated • Unsuitable for large-scale separation of pure CDs	Hg^{2+}, uric acid sensing, α-amanitin in serum detection, catalytic reduction, fluorescent inks, *in vitro* & *in vivo* imaging in the presence of highly reactive oxygen species, anti-bacterial & cyto-toxicity assays, & fabrication of solar cells
Solvent extraction	Separating funnel or separating column	Transfer of CDs and impurities based on their solubility in two immiscible solvents	• Relatively simple • CDs transferred to miscible solvents show characteristic PL properties	• Separation of two-component systems rather than multi-component ones • Separated solutions may contain more than one type of species • Cannot separate CDs of the same type with another	Hg^{2+} & Fe^{3+} sensing in water, cell imaging & photo-catlytic removal of organic pollutants from water
Gradient extraction	Separating funnel	Separation of CD fractions with gradient surface polarities with increase in polarity of the extraction solvent	• Simple and cheap	• Selection of solvents based on the surface functional groups • Cannot separate CDs and impurities with similar surface polarities	—

Table 1 *(Contd.)*

Purification method	Separation device	Separation principle	Advantages	Challenges	Analytical applications
Cloud point extraction	Centrifuge tubes	Separation based on pH-induced polarity changes of CDs	• Simple, inexpensive, fast, and green method • Potential use for large-scale separation of pure CDs • Excludes any toxic solvents or reagents • Can separate CDs into fractions of uniform optical behavior	—	—
SEC	Column/reversed phase/anionic exchange/HPLC systems	Inclusion or exclusion of CDs from the pores within the gel matrix based on size	• Conditions can be varied to suit the type of CD sample or further purification, analysis, or storage requirements	• Needs optimisation of conditions to achieve sufficient selectivity	*In vitro* & *in vivo* imaging, cytotoxicity assays
HPLC		Distribution of compounds between mobile and stationary phases	High peak resolution Collection of CD fractions with scale-up capabilities	High cost Solvents and columns are expensive Regular maintenance and calibration needed	—
UHPLC		Separates components of a mixture by using high pressure to push solvents through the column	• Shorter retention time and better resolution • Superior to HPLC in terms of efficiency, sample loading, separation speed, and solvent consumption	• Small sample loading • Less collected CD fractions are insufficient for further characterization • Higher concentration and larger sample size loading may lead to peak broadening and tailing, resulting in poor separation of CD fractions	—
AE-HPLC		Separation of negatively charged ions/molecules/CDs based on their affinity for positively charged stationary phase groups of the ion exchange resin	• High-resolution analysis • Separation of negatively charged CDs • Significant amounts of CDs can be collected • Provides valuable insight into the complexity and composition of the CD sample • Separates charged species to facilitate studies on the influence of surface charge on PL features	• Separates charged components, and not suitable to handle neutral CDs • Fraction collection is time-consuming	—
RP-HPLC		Separation based on the more polar mobile phase compared with stationary phase	• Can deal with a complex mixture of both charged and neutral CDs • More popular compared with AE-HPLC due to higher separation efficiency, but less expensive	• Unable to separate highly polar or ionic compounds from the column void volume, but retaining good peak symmetry	Cytotoxicity assay & bioimaging
Gravity chromatography		Adsorption of CD solution using a stationary phase and separation into discrete components based on polarity difference	• Simple and used for laboratory-scale separation • Involves minimal instrumentation	• Slow and time-consuming • Manual process requires constant monitoring • Not a high-resolution technique • Reproducibility issue if care is not taken to normalize methods • Optimisation of sample loading and adjusting the flow rate	—

Table 1 *(Contd.)*

Purification method	Separation device	Separation principle	Advantages	Challenges	Analytical applications
GE	GE system	Mobility of bands and segregation of components by charge-to-size ratio under the influence of an electric field. Smaller and oppositely charged species migrate at a faster rate than larger species	• Efficient physical separation of constituents • Requires only a small amount of sample (20–30 μL) • Separated components can easily be physically extracted by cutting the gel and washing out the samples or by freeze-drying	• Large-scale separations not possible; need for scale up • Limited application in the separation of CDs with a wide range of size	Bioimaging of A549 & BHK-21 cells
CZE	Fused silica capillary and electrophoresis unit	Different electrophoretic mobilities based on charge/size ratio through an electrolyte contained in a fused silica capillary under an electric field	• Good separation efficiency • Simple to perform • Separates positively, neutral and negatively charged CDs simultaneously	• Low sensitivity of UV detection systems due to low sample injection volumes • Collection of sufficient amounts of CD fractions is extremely time-consuming • Can separate only the charged CDs rather than the neutral ones, which elute out as one single intense peak	Ketamine detection

CD species. For instance, a less understood structure and relatively low fluorescence QY are the major drawbacks that restrict their usage in the life sciences. Moreover, highly fluorescent molecular fluorophores can also contribute to the PL properties along with CDs, leading to inconsistent, erroneous results and interpretation of data. The review provides clear evidence that the fluorescent impurities and byproducts produced during the synthesis of CDs must be completely removed to achieve reliable results. Although TEM/AFM cannot serve the purpose, a few characterisation approaches such as NMR spectroscopy and MS can help detect the presence of these fluorophores.

The true chemical nature and insights into the origin of PL properties can be comprehended only upon obtaining pure CDs, devoid of various impurities. Therefore, a careful separation of various CD fractions, which can be confirmed by MALDI-TOF MS and TEM techniques, is vital for structural analysis. The morphology, chemical composition, and fundamental properties of CDs can be better understood to establish their applications in different fields. The isolation of pure homogeneous fluorescent CDs could significantly increase the QY, sensitivity, and, consequently, the operational efficiency of CD-based nanosensors. In contrast to the top-down synthesis of CDs that is associated with fewer molecular byproducts, the fluorescence emission of CDs is dominated by the contribution from small molecular weight organic fluorophores in the case of unpurified product samples obtained by bottom-up methods. The unaccounted presence of these organic molecular fluorophores will have a pronounced effect on the fluorescence-based applications of CDs including heavy metal detection, nanosensors and cellular imaging. Though many reports demonstrate centrifugation and filtration for the purification of CDs, these methods have been frequently demonstrated as inadequate separation techniques. Moreover, performing dialysis with inappropriate membranes with too low an MWCO or adopting a shorter procedure duration results in incomplete purification. In addition, the complete removal of fluorescent byproducts formed alongside the CDs is not guaranteed even when performing dialysis with a membrane MWCO of 50 kDa. Thus, the complex and multicomponent nature of the as-synthesized CDs suggests that dialysis, despite its convenience, may not be a satisfactory mode of purification in some instances. The complete removal of fluorophores might require using more than one technique.

Based on previous reports, studies focussing on analytical separation techniques of CDs are limited. A few researchers have used the most analytically sound chromatographic techniques to reduce the CD mixture complexity through fractionation, but these reports currently constitute only <10% of the reported CD purification protocols. Though robust HPLC- or AE-HPLC-assisted separation techniques that can fractionate CDs may benefit in evaluating the synthetic parameters and product generated, the scale-up ability of this process to the preparative range is an attractive opportunity to attain homogeneous fluorescent CDs in milligram quantities for a wide range of applications. Although AE-HPLC is used to separate

negatively charged nanocarbon species, cation-exchange HPLC could be a similar applicable tool for positively charged CDs. Such separations are increasingly important as it becomes more apparent that surface charge rather than size can be a more effective norm for the favourable fractionation of CDs. Furthermore, although the separations obtained during electrophoresis cannot be obtained on a large scale, the sensitivity to both size and charge in nanoscale systems can provide insights into the kinds of fluorophore generated and, hence, demands a scale-up process. Although individual CD fractions that showcase distinct optical properties from the as-synthesized sample including excitation-wavelength-independent emission and QY are realised, a scalable, vetted separation process to achieve CDs of high purity for practical applications remains an unmet challenge.

Several techniques are adopted for the purification of CDs, such as filtration, centrifugation, solvent extraction, dialysis, and chromatography techniques. Various reports state the use of a dialysis method followed by centrifugation and filtration owing to its lesser requirement for technical skills. Filtration is a less time-consuming technique, but the separation of nanoparticles is not explicit and bigger particles tend to clog the pores of the filter. Centrifugation offers a better separation of smaller sized particles as bigger sediments settle at the bottom and less dense particles remain in the supernatant. However, recent studies reveal that smaller sized fluorophores cannot be separated by this method. Dialysis is extensively used as it offers a better separation of smaller sized CDs from larger nanoparticles. The utmost importance lies in the use of appropriate molecular weight cut-off dialysis bags, and hydrophobic CDs cannot be separated by this technique. The solvent extraction method is useful to separate amphiphilic CDs from the hydrophobic components. It is a relatively simpler method used in the separation of two-component/species systems. Column chromatography techniques are less explored and can offer a better alternative for the separation of multi-component CDs with better accuracy. A size-exclusion based column ensures the size-based separation of nanoparticles. High- and ultra-high-performance chromatography can be used in large-scale purification with a shorter elution time and better resolution. The regular optimisation and maintenance along with the high cost limit its application.

Though the PL mechanism and application of CDs are thoroughly investigated, the impact of purification on the emission characteristics of CDs needs to be explored further. Moreover, the use of different precursors introduces uncertainty and therefore, a unified methodology and not an absolute standard protocol has to be adopted for the purification and separation of the CD sample. The sole reason that the as-synthesized CDs are complex mixtures which are far ideal in terms of purity leaves plenty of room for sound analytical separation approaches to harvest precise CD fractions for target applications. There is an urgent need for quality fundamental studies on the purification and separation of CDs and the emission features that vary with size, surface charge, presence of heteroatoms *etc.*, but are unique to a specific CD fraction with a homogeneous composition. Efficient analytical separation techniques must be developed to isolate high-purity CD fractions with unique physicochemical properties. The next step in the research related to carbonaceous nanomaterials should be aimed at a complete shift towards the synthesis of engineered CDs for targeted real-life utility, which calls for an in depth understanding not only of the chemical composition of the final product and its optical properties, but also to establish a clear relationship between the precursor materials used and the reaction conditions. Thus, rigorous and consistent purification steps need to be uniformly implemented, facilitating a tactical change that will unlock the full potential of these carbonaceous nanoparticles as next-generation smart materials for full-color solid-state lighting, photovoltaics, catalysis, biological imaging and sensing.

Abbreviations

AE-HPLC	Anion-exchange high-performance liquid chromatography
AFM	Atomic force microscope
CDs	Carbon dots
CNDs	Carbon nanodots
CPDs	Carbonized polymer dots
CQDs	Carbon quantum dots
CZE	Capillary zone electrophoresis
GE	Gel electrophoresis
GQDs	Graphene quantum dots
HMF	5-(Hydroxymethyl)furfural
HOMO	Highest occupied molecular orbital
HPLC	High-performance liquid chromatography
HPPT	4-Hydroxy-1*H*-pyrrolo[3,4-*c*]pyridine-1,3,6(2*H*,5*H*)-trione
IPCA	Imidazo[1,2-*a*]pyridine-7-carboxylic acid
LUMO	Lowest unoccupied molecular orbital
MS	Mass spectrometry
MWCO	Molecular weight cut-off
N	Nitrogen
NIR	Near-infrared
NMR	Nuclear magnetic resonance
PAGE	Polyacrylamide gel electrophoresis
PL	Photoluminescence
RP-HPLC	Reversed-phase high-performance liquid chromatography
SDGC	Sucrose density gradient centrifugation
SDS	Sodium dodecyl sulfate
SEC	Size exclusion chromatography
TEM	Transmission electron microscope
TPCA	5-Oxo-3,5-dihydro-2*H*-thiazolo[3,2-*a*]pyridine-7-carboxylic acid
TPDCA	5-Oxo-3,5-dihydro-2*H*-thiazolo[3,2-*a*]pyridine-3,7-dicarboxylic acid
UHPLC	Ultra-high-performance liquid chromatography
UV	Ultraviolet
QY	Quantum yield

Conflicts of interest

There are no conflicts to declare.

References

1 X. Xu, R. Ray, Y. Gu, H. J. Ploehn, L. Gearheart, K. Raker and W. A. Scrivens, *J. Am. Chem. Soc.*, 2004, **126**, 12736–12737.
2 J. Wang, R. Sheng Li, H. Zhi Zhang, N. Wang, Z. Zhang and C. Z. Huang, *Biosens. Bioelectron.*, 2017, **97**, 157–163.
3 J. Jana, H. J. Lee, J. S. Chung, M. H. Kim and S. H. Hur, *Anal. Chim. Acta*, 2019, **1079**, 212–219.
4 J. Hu, F. Tang, Y.-Z. Jiang and C. Liu, *Analyst*, 2020, **145**, 2184–2190.
5 M. L. Liu, B. Bin Chen, C. M. Li and C. Z. Huang, *Green Chem.*, 2019, **21**, 449–471.
6 K. Qin, D. Zhang, Y. Ding, X. Zheng, Y. Xiang, J. Hua, Q. Zhang, X. Ji, B. Li and Y. Wei, *Analyst*, 2019, **145**, 177–183.
7 L. Cui, J. Wang and M. Sun, *Rev. Phys.*, 2021, **6**, 100054.
8 F. Yuan, Y. K. Wang, G. Sharma, Y. Dong, X. Zheng, P. Li, A. Johnston, G. Bappi, J. Z. Fan, H. Kung, B. Chen, M. I. Saidaminov, K. Singh, O. Voznyy, O. M. Bakr, Z. H. Lu and E. H. Sargent, *Nat. Photonics*, 2019, **14**, 171–176.
9 C. Hu, M. Li, J. Qiu and Y. P. Sun, *Chem. Soc. Rev.*, 2019, **48**, 2315–2337.
10 Y. Cao, Y. Cheng and M. Sun, *Appl. Spectrosc. Rev.*, 2023, **58**, 1–38.
11 H. Li, X. He, Z. Kang, H. Huang, Y. Liu, J. Liu, S. Lian, C. H. A. Tsang, X. Yang and S. T. Lee, *Angew. Chem., Int. Ed.*, 2010, **49**, 4430–4434.
12 D. Pan, J. Zhang, Z. Li and M. Wu, *Adv. Mater.*, 2010, **22**, 734–738.
13 C. Lee, W. Kwon, S. Beack, D. Lee, Y. Park, H. Kim, S. K. Hahn, S. W. Rhee and C. Kim, *Theranostics*, 2016, **6**, 2196–2208.
14 J. Xia, S. Chen, G. Y. Zou, Y. L. Yu and J. H. Wang, *Nanoscale*, 2018, **10**, 22484–22492.
15 C. Xia, S. Zhu, T. Feng, M. Yang, B. Yang, C. Xia, T. Feng, M. Yang, B. Yang and S. Zhu, *Adv. Sci.*, 2019, **6**, 1901316.
16 S. Mandal and P. Das, *Appl. Mater. Today*, 2022, **26**, 101331.
17 S. Zhu, J. Zhang, L. Wang, Y. Song, G. Zhang, H. Wang and B. Yang, *Chem. Commun.*, 2012, **48**, 10889–10891.
18 R. Tabaraki and O. Abdi, *J. Fluoresc.*, 2019, **29**, 751–756.
19 M. Tian, Y. Wang and Y. Zhang, *J. Nanosci. Nanotechnol.*, 2018, **18**, 8111–8117.
20 J. Luo, Z. Sun, W. Zhou, F. Mo, Z. chao Wu and X. Zhang, *Opt. Mater.*, 2021, **113**, 110796.
21 C. Li, X. Sun, Y. Li, H. Liu, B. Long, D. Xie, J. Chen and K. Wang, *ACS Omega*, 2021, **6**, 3232–3237.
22 Y. Liu, H. Huang, W. Cao, B. Mao, Y. Liu and Z. Kang, *Mater. Chem. Front.*, 2020, **4**, 1586–1613.
23 M. Pirsaheb, S. Mohammadi and A. Salimi, *TrAC, Trends Anal. Chem.*, 2019, **115**, 83–99.
24 H. Barhum, T. Alon, M. Attrash, A. Machnev, I. Shishkin and P. Ginzburg, *ACS Appl. Nano Mater.*, 2021, **4**, 9919–9931.
25 W. Shi, H. Lv, S. Yuan, H. Huang, Y. Liu and Z. Kang, *Sep. Purif. Technol.*, 2017, **174**, 282–289.
26 X. He, P. Chen, J. Zhang, T. Y. Luo, H. J. Wang, Y. H. Liu and X. Q. Yu, *Biomater. Sci.*, 2019, **7**, 1940–1948.
27 J. Peng, W. Gao, B. K. Gupta, Z. Liu, R. Romero-Aburto, L. Ge, L. Song, L. B. Alemany, X. Zhan, G. Gao, S. A. Vithayathil, B. A. Kaipparettu, A. A. Marti, T. Hayashi, J. J. Zhu and P. M. Ajayan, *Nano Lett.*, 2012, **12**, 844–849.
28 P. Zhao, M. Yang, W. Fan, X. Wang, F. Tang, C. Yang, X. Dou, S. Li, Y. Wang and Y. Cao, *Part. Part. Syst. Charact.*, 2016, **33**, 635–644.
29 W. Shi, Q. Han, J. Wu, C. Ji, Y. Zhou, S. Li, L. Gao, R. M. Leblanc and Z. Peng, *Int. J. Mol. Sci.*, 2022, **23**, 1456.
30 X. Li, H. Wang, Y. Shimizu, A. Pyatenko, K. Kawaguchi and N. Koshizaki, *Chem. Commun.*, 2010, **47**, 932–934.
31 S. Y. Park, H. U. Lee, E. S. Park, S. C. Lee, J. W. Lee, S. W. Jeong, C. H. Kim, Y. C. Lee, Y. S. Huh and J. Lee, *ACS Appl. Mater. Interfaces*, 2014, **6**, 3365–3370.
32 S. Mitra, S. Chandra, S. H. Pathan, N. Sikdar, P. Pramanik and A. Goswami, *RSC Adv.*, 2013, **3**, 3189–3193.
33 Q. Wang, X. Liu, L. Zhang and Y. Lv, *Analyst*, 2012, **137**, 5392–5397.
34 M. K. Kumawat, R. Srivastava, M. Thakur and R. B. Gurung, *ACS Sustainable Chem. Eng.*, 2017, **5**, 1382–1391.
35 M. Xue, Z. Zhan, M. Zou, L. Zhang and S. Zhao, *New J. Chem.*, 2016, **40**, 1698–1703.
36 B. Yin, J. Deng, X. Peng, Q. Long, J. Zhao, Q. Lu, Q. Chen, H. Li, H. Tang, Y. Zhang and S. Yao, *Analyst*, 2013, **138**, 6551–6557.
37 L. Cui, X. Ren, M. Sun, H. Liu and L. Xia, *Nanomaterials*, 2021, **11**, 3419.
38 G. Ge, L. Li, D. Wang, M. Chen, Z. Zeng, W. Xiong, X. Wu and C. Guo, *J. Mater. Chem. B*, 2021, **9**, 6553–6575.
39 Y. Wang and A. Hu, *J. Mater. Chem. C*, 2014, **2**, 6921–6939.
40 S. Schenker, C. Heinemann, M. Huber, R. Pompizzi, R. Perren and F. Escher, *J. Food Sci.*, 2002, **67**, 60–66.
41 T. S. Samaras, P. A. Camburn, S. X. Chandra, M. H. Gordon and J. M. Ames, *J. Agric. Food Chem.*, 2005, **53**, 8068–8074.
42 D. O. Carvalho, L. H. Øgendal, M. L. Andersen and L. F. Guido, *Eur. Food Res. Technol.*, 2016, **242**, 1545–1553.
43 H. Yahya, R. S. T. Linforth and D. J. Cook, *Food Chem.*, 2014, **145**, 378–387.
44 H. X. Wang, Z. Yang, Z. G. Liu, J. Y. Wan, J. Xiao and H. L. Zhang, *Chem. – Eur. J.*, 2016, **22**, 8096–8104.
45 S. Y. Lim, W. Shen and Z. Gao, *Chem. Soc. Rev.*, 2014, **44**, 362–381.
46 K. J. Mintz, Y. Zhou and R. M. Leblanc, *Nanoscale*, 2019, **11**, 4634–4652.

47 Y. P. Sun, B. Zhou, Y. Lin, W. Wang, K. A. S. Fernando, P. Pathak, M. J. Meziani, B. A. Harruff, X. Wang, H. Wang, P. G. Luo, H. Yang, M. E. Kose, B. Chen, L. M. Veca and S. Y. Xie, *J. Am. Chem. Soc.*, 2006, **128**, 7756–7757.
48 X. Yan, B. Li and L. S. Li, *Acc. Chem. Res.*, 2013, **46**, 2254–2262.
49 S. Kim, S. W. Hwang, M. K. Kim, D. Y. Shin, D. H. Shin, C. O. Kim, S. B. Yang, J. H. Park, E. Hwang, S. H. Choi, G. Ko, S. Sim, C. Sone, H. J. Choi, S. Bae and B. H. Hong, *ACS Nano*, 2012, **6**, 8203–8208.
50 F. Yuan, Z. Wang, X. Li, Y. Li, Z. Tan, L. Fan and S. Yang, *Adv. Mater.*, 2017, **29**, 1604436.
51 Z. Tian, X. Zhang, D. Li, D. Zhou, P. Jing, D. Shen, S. Qu, R. Zboril and A. L. Rogach, *Adv. Opt. Mater.*, 2017, **5**, 1700416.
52 K. Jiang, X. Feng, X. Gao, Y. Wang, C. Cai, Z. Li and H. Lin, *Nanomaterials*, 2019, **9**, 529.
53 L. Cao, M. J. Meziani, S. Sahu and Y. P. Sun, *Acc. Chem. Res.*, 2013, **46**, 171–182.
54 L. Wang, S. J. Zhu, H. Y. Wang, S. N. Qu, Y. L. Zhang, J. H. Zhang, Q. D. Chen, H. L. Xu, W. Han, B. Yang and H. B. Sun, *ACS Nano*, 2014, **8**, 2541–2547.
55 Y. Zhang, R. Yuan, M. He, G. Hu, J. Jiang, T. Xu, L. Zhou, W. Chen, W. Xiang and X. Liang, *Nanoscale*, 2017, **9**, 17849–17858.
56 L. Bao, Z. L. Zhang, Z. Q. Tian, L. Zhang, C. Liu, Y. Lin, B. Qi and D. W. Pang, *Adv. Mater.*, 2011, **23**, 5801–5806.
57 H. Ding, S. B. Yu, J. S. Wei and H. M. Xiong, *ACS Nano*, 2016, **10**, 484–491.
58 M. L. Liu, L. Yang, R. S. Li, B. Bin Chen, H. Liu and C. Z. Huang, *Green Chem.*, 2017, **19**, 3611–3617.
59 H. Liu, Z. He, L. P. Jiang and J. J. Zhu, *ACS Appl. Mater. Interfaces*, 2015, **7**, 4913–4920.
60 X. Miao, D. Qu, D. Yang, B. Nie, Y. Zhao, H. Fan and Z. Sun, *Adv. Mater.*, 2018, **30**, 1704740.
61 S. Zhu, Y. Song, J. Wang, H. Wan, Y. Zhang, Y. Ning and B. Yang, *Nano Today*, 2017, **13**, 10–14.
62 L. Bao, C. Liu, Z. L. Zhang and D. W. Pang, *Adv. Mater.*, 2015, **27**, 1663–1667.
63 Z. Liu, H. Zou, N. Wang, T. Yang, Z. Peng, J. Wang, N. Li and C. Huang, *Sci. China: Chem.*, 2018, **61**, 490–496.
64 Y. Xiong, J. Schneider, C. J. Reckmeier, H. Huang, P. Kasák and A. L. Rogach, *Nanoscale*, 2017, **9**, 11730–11738.
65 W. Wang, B. Wang, H. Embrechts, C. Damm, A. Cadranel, V. Strauss, M. Distaso, V. Hinterberger, D. M. Guldi and W. Peukert, *RSC Adv.*, 2017, **7**, 24771–24780.
66 M. J. Krysmann, A. Kelarakis, P. Dallas and E. P. Giannelis, *J. Am. Chem. Soc.*, 2012, **134**, 747–750.
67 P. Duan, B. Zhi, L. Coburn, C. L. Haynes and K. Schmidt-Rohr, *Magn. Reson. Chem.*, 2020, **58**, 1130–1138.
68 J. Schneider, C. J. Reckmeier, Y. Xiong, M. Von Seckendorff, A. S. Susha, P. Kasak and A. L. Rogach, *J. Phys. Chem. C*, 2017, **121**, 2014–2022.
69 J. B. Essner, J. A. Kist, L. Polo-Parada and G. A. Baker, *Chem. Mater.*, 2018, **30**, 1878–1887.
70 M. Righetto, A. Privitera, I. Fortunati, D. Mosconi, M. Zerbetto, M. L. Curri, M. Corricelli, A. Moretto, S. Agnoli, L. Franco, R. Bozio and C. Ferrante, *J. Phys. Chem. Lett.*, 2017, **8**, 2236–2242.
71 L. Shi, J. H. Yang, H. B. Zeng, Y. M. Chen, S. C. Yang, C. Wu, H. Zeng, O. Yoshihito and Q. Zhang, *Nanoscale*, 2016, **8**, 14374–14378.
72 S. Zhu, X. Zhao, Y. Song, S. Lu and B. Yang, *Nano Today*, 2016, **11**, 128–132.
73 Y. Song, S. Zhu, S. Zhang, Y. Fu, L. Wang, X. Zhao and B. Yang, *J. Mater. Chem. C*, 2015, **3**, 5976–5984.
74 V. Gude, A. Das, T. Chatterjee and P. K. Mandal, *Phys. Chem. Chem. Phys.*, 2016, **18**, 28274–28280.
75 W. Kasprzyk, T. Świergosz, S. Bednarz, K. Walas, N. V. Bashmakova and D. Bogdał, *Nanoscale*, 2018, **10**, 13889–13894.
76 A. Das, V. Gude, D. Roy, T. Chatterjee, C. K. De and P. K. Mandal, *J. Phys. Chem. C*, 2017, **121**, 9634–9641.
77 X. Yao, Y. Wang, F. Li, J. J. Dalluge, G. Orr, R. Hernandez, Q. Cui and C. L. Haynes, *Nanoscale*, 2022, **14**, 9516–9525.
78 W. Zhang, X. Fang, F. He, J. Bai, Y. Cheng, K. Weerasinghe, X. Meng, H. Xu and T. Ding, *J. Phys. Chem. C*, 2021, **125**, 5207–5216.
79 B. Bartolomei and M. Prato, *Small*, 2023, **19**, 2206714.
80 Y. Xiong, J. Schneider, E. V. Ushakova and A. L. Rogach, *Nano Today*, 2018, **23**, 124–139.
81 C. J. Reckmeier, J. Schneider, Y. Xiong, J. Häusler, P. Kasák, W. Schnick and A. L. Rogach, *Chem. Mater.*, 2017, **29**, 10352–10361.
82 S. Khan, A. Sharma, S. Ghoshal, S. Jain, M. K. Hazra and C. K. Nandi, *Chem. Sci.*, 2017, **9**, 175–180.
83 B. Bartolomei, A. Bogo, F. Amato, G. Ragazzon and M. Prato, *Angew. Chem., Int. Ed.*, 2022, **61**, e202200038.
84 D. Sun, R. Ban, P. H. Zhang, G. H. Wu, J. R. Zhang and J. J. Zhu, *Carbon*, 2013, **64**, 424–434.
85 M. Lan, J. Zhang, Y. S. Chui, H. Wang, Q. Yang, X. Zhu, H. Wei, W. Liu, J. Ge, P. Wang, X. Chen, C. S. Lee and W. Zhang, *J. Mater. Chem. B*, 2014, **3**, 127–134.
86 Y. Choi, G. H. Ryu, S. H. Min, B. R. Lee, M. H. Song, Z. Lee and B. S. Kim, *ACS Nano*, 2014, **8**, 11377–11385.
87 S. Chandra, P. Das, S. Bag, D. Laha and P. Pramanik, *Nanoscale*, 2011, **3**, 1533–1540.
88 P. C. Hsu, Z. Y. Shih, C. H. Lee and H. T. Chang, *Green Chem.*, 2012, **14**, 917–920.
89 M. X. Gao, C. F. Liu, Z. L. Wu, Q. L. Zeng, X. X. Yang, W. B. Wu, Y. F. Li and C. Z. Huang, *Chem. Commun.*, 2013, **49**, 8015–8017.
90 S. S. Liu, C. F. Wang, C. X. Li, J. Wang, L. H. Mao and S. Chen, *J. Mater. Chem. C*, 2014, **2**, 6477–6483.
91 S. Xie, H. Su, W. Wei, M. Li, Y. Tong and Z. Mao, *J. Mater. Chem. A*, 2014, **2**, 16365–16368.
92 K. Wei, J. Li, Z. Ge, Y. You and H. Xu, *RSC Adv.*, 2014, **4**, 52230–52234.
93 S. Pandey, A. Mewada, G. Oza, M. Thakur, N. Mishra, M. Sharon and M. Sharon, *Nanosci. Nanotechnol. Lett.*, 2013, **5**, 775–779.

94 Q. Hu, X. Gong, L. Liu and M. M. F. Choi, *J. Nanomater.*, 2017, 1804178, DOI: **10.1155/2017/1804178**.
95 S. Sahu, B. Behera, T. K. Maiti and S. Mohapatra, *Chem. Commun.*, 2012, **48**, 8835–8837.
96 L. Deng, X. Wang, Y. Kuang, C. Wang, L. Luo, F. Wang and X. Sun, *Nano Res.*, 2015, **8**, 2810–2821.
97 S. D. Dsouza, M. Buerkle, P. Brunet, C. Maddi, D. B. Padmanaban, A. Morelli, A. F. Payam, P. Maguire, D. Mariotti and V. Svrcek, *Carbon*, 2021, **183**, 1–11.
98 R. Liu, H. Li, W. Kong, J. Liu, Y. Liu, C. Tong, X. Zhang and Z. Kang, *Mater. Res. Bull.*, 2013, **48**, 2529–2534.
99 R. Liu, J. Liu, W. Kong, H. Huang, X. Han, X. Zhang, Y. Liu and Z. Kang, *Dalton Trans.*, 2014, **43**, 10920–10929.
100 B. Wang, A. Song, L. Feng, H. Ruan, H. Li, S. Dong and J. Hao, *ACS Appl. Mater. Interfaces*, 2015, **7**, 6919–6925.
101 H. Zhang, P. Dai, L. Huang, Y. Huang, Q. Huang, W. Zhang, C. Wei and S. Hu, *Anal. Methods*, 2014, **6**, 2687–2691.
102 E. Ju, Z. Liu, Y. Du, Y. Tao, J. Ren and X. Qu, *ACS Nano*, 2014, **8**, 6014–6023.
103 Y. Yan, W. Kuang, L. Shi, X. Ye, Y. Yang, X. Xie, Q. Shi and S. Tan, *J. Alloys Compd.*, 2019, **777**, 234–243.
104 J. J. Huang, Z. F. Zhong, M. Z. Rong, X. Zhou, X. D. Chen and M. Q. Zhang, *Carbon*, 2014, **70**, 190–198.
105 C. Yuan, B. Liu, F. Liu, M. Y. Han and Z. Zhang, *Anal. Chem.*, 2014, **86**, 1123–1130.
106 L. Feng, L. Tan, H. Li, Z. Xu, G. Shen and Y. Tang, *Biosens. Bioelectron.*, 2015, **69**, 265–271.
107 F. Noun, J. Manioudakis and R. Naccache, *Part. Part. Syst. Charact.*, 2020, **37**, 2000119.
108 Q. Zhang, X. Sun, H. Ruan, K. Yin and H. Li, *Sci. China Mater.*, 2017, **60**, 141–150.
109 C. Y. Chen, Y. H. Tsai and C. W. Chang, *New J. Chem.*, 2019, **43**, 6153–6159.
110 H. M. R. Gonçalves, A. J. Duarte and J. C. G. Esteves da Silva, *Biosens. Bioelectron.*, 2010, **26**, 1302–1306.
111 S. Mitra, S. Chandra, T. Kundu, R. Banerjee, P. Pramanik and A. Goswami, *RSC Adv.*, 2012, **2**, 12129–12131.
112 J. F. Y. Fong, S. F. Chin and S. M. Ng, *Sens. Actuators, B*, 2015, **209**, 997–1004.
113 P. Zhang, W. Li, X. Zhai, C. Liu, L. Dai and W. Liu, *Chem. Commun.*, 2012, **48**, 10431–10433.
114 B. Y. Yu and S. Y. Kwak, *J. Mater. Chem.*, 2012, **22**, 8345–8353.
115 J. Wang, C. Cheng, Y. Huang, B. Zheng, H. Yuan, L. Bo, M.-W. Zheng, S.-Y. Yang, Y. Guo and D. Xiao, *J. Mater. Chem. C*, 2014, **2**, 5028–5035.
116 J. Zhu, C. Wu, Y. Cui, D. Li, Y. Zhang, J. Xu, C. Li, S. Iqbal and M. Cao, *Colloids Surf., A*, 2021, **623**, 126673.
117 S. Han, H. Zhang, J. Zhang, Y. Xie, L. Liu, H. Wang, X. Li, W. Liu and Y. Tang, *RSC Adv.*, 2014, **4**, 58084–58089.
118 A. Beiraghi and S. A. Najibi-Gehraz, *J. Nanostruct.*, 2020, **10**, 107–118.
119 O. E. Trubetskaya, O. A. Trubetskoj, C. Richard, A. M. Vervald, S. A. Burikov, V. V. Marchenkov, O. A. Shenderova, S. V. Patsaeva and T. A. Dolenko, *J. Chromatogr. A*, 2021, **1650**, 462251.
120 X. Wang, L. Cao, S. T. Yang, F. Lu, M. J. Meziani, L. Tian, K. W. Sun, M. A. Bloodgood and Y. P. Sun, *Angew. Chem., Int. Ed.*, 2010, **49**, 5310–5314.
121 C. Jiang, H. Wu, X. Song, X. Ma, J. Wang and M. Tan, *Talanta*, 2014, **127**, 68–74.
122 D. D. Liu, H. Su, Q. Cao, X. Y. Le and Z. W. Mao, *RSC Adv.*, 2015, **5**, 40588–40594.
123 N. Fuyuno, D. Kozawa, Y. Miyauchi, S. Mouri, R. Kitaura, H. Shinohara, T. Yasuda, N. Komatsu and K. Matsuda, *Adv. Opt. Mater.*, 2014, **2**, 983–989.
124 X. Gong, M. Chin Paau, Q. Hu, S. Shuang, C. Dong and M. M. F. Choi, *Talanta*, 2016, **146**, 340–350.
125 J. C. Vinci and L. A. Colon, *Anal. Chem.*, 2012, **84**, 1178–1183.
126 J. C. Vinci, I. M. Ferrer, S. J. Seedhouse, A. K. Bourdon, J. M. Reynard, B. A. Foster, F. V. Bright and L. A. Colón, *J. Phys. Chem. Lett.*, 2013, **4**, 239–243.
127 J. C. Vinci and L. A. Colón, *Microchem. J.*, 2013, **110**, 660–664.
128 X. Gong, Q. Hu, M. Chin Paau, Y. Zhang, L. Zhang, S. Shuang, C. Dong and M. M. F. Choi, *Talanta*, 2014, **129**, 529–538.
129 Q. Hu, M. C. Paau, M. M. F. Choi, Y. Zhang, X. Gong, L. Zhang, Y. Liu and J. Yao, *Electrophoresis*, 2014, **35**, 2454–2462.
130 X. Gong, Q. Hu, M. C. Paau, Y. Zhang, S. Shuang, C. Dong and M. M. F. Choi, *Nanoscale*, 2014, **6**, 8162–8170.
131 V. Hinterberger, C. Damm, P. Haines, D. M. Guldi and W. Peukert, *Nanoscale*, 2019, **11**, 8464–8474.
132 H. Liu, T. Ye and C. Mao, *Angew. Chem., Int. Ed.*, 2007, **46**, 6473–6475.
133 A. A. Kokorina, A. A. Bakal, D. V. Shpuntova, A. Y. Kostritskiy, N. V. Beloglazova, S. De Saeger, G. B. Sukhorukov, A. V. Sapelkin and I. Y. Goryacheva, *Sci. Rep.*, 2019, **9**, 1–8.
134 A. Sachdev, I. Matai and P. Gopinath, *RSC Adv.*, 2014, **4**, 20915–20921.
135 J. S. Baker and L. A. Colón, *J. Chromatogr. A*, 2009, **1216**, 9048–9054.
136 H. P. Jen, Y. C. Tsai, H. L. Su and Y. Z. Hsieh, *J. Chromatogr. A*, 2006, **1111**, 159–165.
137 Q. Hu, M. C. Paau, Y. Zhang, W. Chan, X. Gong, L. Zhang and M. M. F. Choi, *J. Chromatogr. A*, 2013, **1304**, 234–240.
138 Y. Wu and V. T. Remcho, *Talanta*, 2016, **161**, 854–859.